

Provided for non-commercial research and education use.  
Not for reproduction, distribution or commercial use.



This article appeared in a journal published by Elsevier. The attached copy is furnished to the author for internal non-commercial research and education use, including for instruction at the authors institution and sharing with colleagues.

Other uses, including reproduction and distribution, or selling or licensing copies, or posting to personal, institutional or third party websites are prohibited.

In most cases authors are permitted to post their version of the article (e.g. in Word or Tex form) to their personal website or institutional repository. Authors requiring further information regarding Elsevier's archiving and manuscript policies are encouraged to visit:

<http://www.elsevier.com/copyright>



ELSEVIER

Available online at [www.sciencedirect.com](http://www.sciencedirect.com)

Remote Sensing of Environment 112 (2008) 2033–2050

---



---

Remote Sensing  
of  
Environment

---



---

[www.elsevier.com/locate/rse](http://www.elsevier.com/locate/rse)

# Habitat selection by a rare forest antelope: A multi-scale approach combining field data and imagery from three sensors

L.D. Estes<sup>a,b,\*</sup>, G.S. Okin<sup>c</sup>, A.G. Mwangi<sup>d</sup>, H.H. Shugart<sup>b</sup>

<sup>a</sup> Rare Species Conservatory Foundation, P.O. Box 1371, Loxahatchee, FL 33470, USA

<sup>b</sup> Center for Regional Environmental Studies, Department of Environmental Science, University of Virginia, 291 McCormick Road Charlottesville, VA 22903, USA

<sup>c</sup> Department of Geography, University of California Los Angeles, Box 951524, Los Angeles, CA 90095, USA

<sup>d</sup> School of Natural Resource Management, Moi University, P.O. Box 3900, 30100 Eldoret, Kenya

Received 2 December 2006; received in revised form 7 January 2008; accepted 9 January 2008

---

## Abstract

It can be difficult to further scientific understanding of rare or endangered species that live in inaccessible habitat using traditional methods, such as probabilistic modeling based on field data collection. Remote sensing (RS) can be an important source of information for the study of these animals. A key advantage of RS is its ability to provide information over an animal's complete range, but models incorporating RS data are limited by RS's ability to detect important habitat features. In this study, we focus on the rare, poorly-understood mountain bongo antelope (*Tragelaphus euryceros isaaci*) which survives in the wild in isolated pockets of montane forest in Kenya. We hypothesize that mountain bongo habitat is multi-scaled. We analyzed field and RS data (derived from SPOT, ASTER, and MODIS) ranging in scale from 0.02–85.93 ha to test our hypothesis. Important microhabitat features were identified through logistic regression models of vegetation structure data collected in plots (0.04 ha) of bongo presence ( $n=36$ ) and absence ( $n=90$ ). Models were selected using an information theoretic approach. We analyzed the correlations between microhabitat (four canopy and four understorey structure measures) and RS variables derived using spectral mixture (SMA) and texture analysis; most ASTER and SPOT variables were significantly related with canopy structure variables ( $\max|r|=0.56$ ), but correlations between understorey structure and all but two RS variables were insignificant. Further logistic regression modeling showed that combining field microhabitat (primarily understorey structure variables) and larger-scaled RS measures (ASTER spectral mixture analysis variables aggregated to 450 m (20.25 ha)) provided superior models of bongo habitat selection than those based on field or RS data only. The results demonstrate that: 1) forest canopy characteristics at scales of ~20 ha and understorey structural conditions at the micro-scale of 0.04 ha were the most important features influencing bongo habitat selection; 2) models for predicting bongo habitat distribution must incorporate both micro- and macro-habitat variables; 3) optical RS data may characterize important micro-scale canopy variables with reasonable accuracy, but are ineffective for detecting understorey features (unless alternative techniques such as forest structural indices can be successfully applied); 4) RS and field data are both essential for understanding bongo habitat selection. The technique employed here for understanding this rare antelope's habitat selection may also be applied in studies of other large herbivores.

© 2008 Elsevier Inc. All rights reserved.

**Keywords:** SPOT; ASTER; MODIS; Spectral mixture analysis; Texture analysis; Topographic correction; Habitat selection; Herbivore; Forest structure; Scale; Field data; Rare species; Mountain bongo; Logistic regression; Akaike's information criterion

## 1. Introduction

Rare species are a preeminent concern of conservation biology, which is the "biology of scarcity" (Soule, 1986, pg. 10). Successfully conserving a rare species depends on understanding interactions between the organism and its environment. Spatially-explicit, probabilistic distribution models are important tools for

---

\* Corresponding author. Center for Regional Environmental Studies, Department of Environmental Science, University of Virginia, 291 McCormick Road Charlottesville, VA 22903, USA. Tel.: +1 202 431 0496; fax: +1 434 924 4761.

E-mail address: [lde2c@virginia.edu](mailto:lde2c@virginia.edu) (L.D. Estes).

examining this relationship, which is central to ecology (Guisan & Zimmermann, 2000). Such models are increasingly used to map species' actual and potential distributions, and to understand the factors influencing these (Guisan & Zimmermann, 2000; Rushton et al., 2004). However, the insight drawn from such models depends on the quality and quantity of input data. Collecting a dataset that is adequate in both senses is difficult when species are rare (Rushton et al., 2004), thus habitat modeling studies are skewed towards more abundant organisms (Guisan et al., 2006).

Rare species pose logistical (cost) and statistical (sample size, independence) problems for distribution modeling studies (Guisan & Zimmermann, 2000; Rushton et al., 2004). Furthermore, predicted distribution patterns and the factors influencing them can vary according to the scale of investigation, as most organisms' habitats are determined by features defined at different scales (Brown, 1995; Wiens, 1989). Choosing appropriate sampling scales is difficult for rare organisms, whose ecological requirements are often poorly-understood (Rushton et al., 2004).

Remote sensing (hereafter RS) is increasingly used in habitat modeling studies to overcome the problems of sample size and scale; RS provides the most efficient technique for collecting large quantities of habitat data over extensive areas at multiple spatial scales (Kerr & Ostrovsky, 2003; Rushton et al., 2004; Turner et al., 2003; Wulder et al., 2004). Modern sensors offer the ability to collect information throughout the electromagnetic spectrum at sub-meter to multi-kilometer resolutions, and can be directly related to a number of field-based ecological measures (Turner et al., 2003). The advances in sensor technology and related analytical techniques have facilitated the increasing use of spatial distribution models in ecological and conservation applications, as high quality data can be collected and meaningfully interpreted in habitats where field surveys are technically or financially impractical (Rushton et al., 2004; Wulder et al., 2004).

Despite this trend, many ecologists and biologists remain skeptical that RS data are suitable for fine-scale ecological studies (Turner et al., 2003). Furthermore, since most sensors are not designed to provide input for distribution models, the ability of RS to detect important habitat features varies according to the characteristics of a species and its ecosystem; these determine whether RS measurements describe the driving habitat variables or their proxies (Rushton et al., 2004; Turner et al., 2003). For instance, high resolution RS data may detect shrubs browsed by an antelope in an open savanna woodland, but would fail to do so if these shrubs were located under closed-canopy forest. In the latter case, the RS data might correlate with a proxy variable, such as canopy cover.

Many RS-based habitat modeling studies rely on such proxies, which are often categorical variables that describe land cover or vegetation types (e.g. Debinski et al., 1999; Saveraid et al., 2001; Schadt et al., 2002). Categorical variables can be poor predictors of the species-habitat relationship, since they cannot account for within-class variability and struggle to distinguish ecotones (St-Louis et al., 2006). More informative proxy variables can be established by developing continuous relationships between RS data and relevant habitat features, such as vegetation structure (Rushton et al., 2004; St-Louis et al.,

2006; Turner et al., 2003). The use of continuous, RS-derived proxies is growing in habitat modeling studies (e.g. Gibson et al., 2004; Jeganathan et al., 2004), but ecologists have yet to embrace many of the techniques developed for quantifying such variables (Turner et al., 2003). For instance, the RS literature contains many studies in which RS is used to measure forest structural variables (Hansen et al., 2001; Hudak et al., 2002; Peddle et al., 2001; Scarth et al., 2001; Wulder et al., 1998; Wulder et al., 2004). These methods could be profitably applied in habitat modeling studies of forest-dwelling species.

The subject of this study is the mountain bongo (*Tragelaphus euryceros isaaci*), a large, elusive antelope endemic to a handful of high mountain forests in Kenya. The mountain bongo (hereafter bongo), a distinctive sub-species of Central and West Africa's lowland bongo (*Tragelaphus euryceros euryceros*), was once abundant in the isolated montane forest patches (see Fig. 1A) that represent the limits of its potential habitat. In the past several decades, however, the number of bongos has declined precipitously. Causes are uncertain, but probably stem from a combination of rampant poaching, human encroachment into Kenya's relatively small forest estate, and diseases such as rinderpest (Gathaara, 1999; Imbernon, 1999; Kock et al., 1999; Lambrechts et al., 2003). Less than 100 individuals are believed to remain in the wild (Prettejohn, 2004; Reillo, 2002), the majority of which are confined to the Aberdare Mountains (Fig. 1B). An international reintroduction and conservation project is now underway, which aims to recover the extant sub-populations and re-establish a viable bongo population on Mount Kenya (Fig. 1B), where one of the largest sub-populations used to be found.

This study is part of the ecological research being conducted to support this broader conservation project, which is crucial because of the near-absence of information on bongo ecology. A primary objective is to determine bongo habitat selection and distribution throughout its range using spatial distribution models. However, obtaining the necessary data for developing these models is extremely difficult given the bongo's rarity; the Aberdares' bongo sub-population is the only one with sufficient numbers to study, yet even this herd's density is low relative to the Aberdares' extensive, rugged forest estate. These conditions make it impractical to obtain the sort of fully-stratified, multi-scale field survey data needed for successful distribution models (Vaughan & Ormerod, 2003), as collecting just one observation requires significant investments in time, money, and labor. Furthermore, choosing appropriate sampling scales is difficult in the absence of prior knowledge, while the high costs of field work preclude exploratory investigations. These factors indicate that the necessary habitat information must be provided by RS data trained with a relatively small field dataset. Unfortunately, montane forests challenge the capabilities of optical RS data (the kind most readily available to conservation ecologists), as forest reflectance received by the sensor is confounded by the variable illumination that results from extreme topography (Gu & Gillespie, 1998).

Existing information on the bongo indicates that it is primarily a browser of forest edge and understorey plants, and its preferred habitat appears to be a mosaic of open glades,

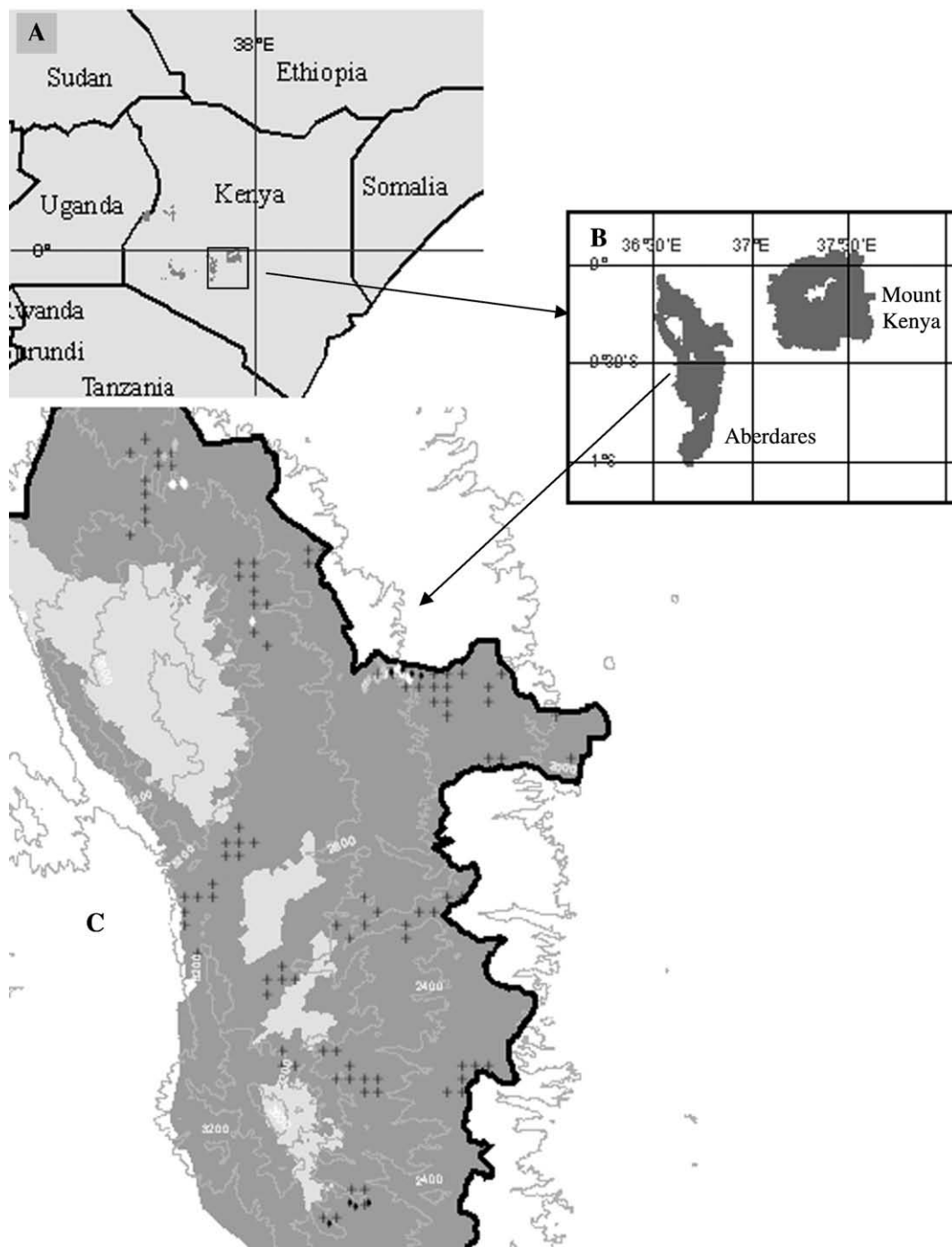


Fig. 1. A) The mountain bongo's potential distribution (dark grey areas) within Kenya. Mount Kenya and the Aberdares fall within the black square. B) The Aberdares in relation to Mount Kenya. C) Detailed view of the Aberdares, with potential bongo habitat shaded dark grey. The position of the fenceline is indicated by the heavy black line. Field sample plot locations are denoted by black diamonds (1st season bongo samples), grey diamonds (2nd season bongo samples), white diamonds (3rd season bongo samples), and black crosses (grid points).

secondary re-growth, and primary forest (Kingdon, 1982). Bongo home ranges may be as large as 120–300 km<sup>2</sup>, and encompass the variety of floristic types represented within the larger montane forest patches (usually 500–1000 km<sup>2</sup>) that delineate the potential habitat of each bongo sub-population (Kingdon, 1982). These characteristics suggest that bongos respond to vegetation structural features (best characterized with continuous variables) more than composition (a categorical

descriptor); canopy structural variations should influence browse and cover abundance more than the type of species forming the canopy. Such structural features are likely to be described by scales ranging from several hundred square meters (e.g. a small glade or tree-fall gap) to hundreds or thousands of hectares (e.g. secondary forest patches containing abundant browse and cover). Multi-scaled habitat selection has been found in other large herbivores, including caribou *Rangifer*

*tarandus* (Johnson et al., 2004; Terry et al., 2000) and moose *Alces alces* (Cassing et al., 2006; Maier et al., 2005), as well as other mobile species, such as porcupine *Erethizon dorsatum* (Morin et al., 2005), red squirrel *Tamiasciurus hudsonicus* (Fisher et al., 2005), and capercaillie *Tetrao urogallus* (Graf et al., 2005).

Based on these insights, we hypothesize that bongo select habitat at multiple spatial scales. In order to address this hypothesis, we employ five datasets representing different spatial scales and levels of detail. The greatest detail is provided by micro-scale vegetation structure data, collected in 22.6 m diameter (0.04 ha) field plots centered on areas defined by bongo presence or absence. The additional datasets comprise four RS images, ranging in spatial resolution from 5–927 m (0.02–86 ha), and varying in spectral resolution from one panchromatic band to nine bands in the visible and near infrared.

In our analysis, we use logistic regression to identify the microhabitat structural variables most influencing bongo habitat selection. We then examine the correlation strength between these features and continuous RS variables derived from spectral mixture analysis (SMA) and texture analysis, which are techniques useful for measuring forest structure and the arrangement of species' habitats (Kayitakire et al., 2006; Lu et al., 2003; Sabol et al., 2002; St-Louis et al., 2006; Theau et al., 2005; Wulder et al., 1998). This step allows us to effectively determine both the physical meaning of the RS data and its usefulness for characterizing the microhabitat features important to bongos. We then use logistic regression to 1) assess the relative ability of each RS dataset to discriminate between bongo and non-bongo habitats, and 2) to determine which combination of data—and therefore which spatial scale(s)—provides the best bongo habitat selection model.

The methods we use to address our hypothesis offer valuable insight into 1) the scale and nature of habitat features selected by bongos, 2) the ability of advanced RS techniques to provide useful predictor variables for modeling bongo habitat selection, and 3) the relative merits of several optical RS datasets and field data for studying a rare organism in a challenging environment. Our procedure is transportable to studies of other large, rare herbivores worldwide.

## 2. Methods

### 2.1. Background

#### 2.1.1. Study area

This study focuses on the Aberdare Mountains (3998 m), home of the largest remaining wild bongo population. The Aberdares comprise an equatorial massif that lies 40 km from the geologically and ecologically similar Mount Kenya (Fig. 1B), which was formed by Miocene and Pliocene-era volcanism and tectonic activity, and shaped by Pleistocene glaciation at higher elevations (Schmitt, 1991).

The Aberdares climate is characterized by two rainy seasons (October–December and March–May) interspersed with dry seasons, reflecting shifts in the Inter-Tropical Convergence zone (Schmitt, 1991). Mean annual rainfall increases from north

(~950 mm) to south (~2,250 mm), where exposure to prevailing Indian Ocean winds is greatest (Schmitt, 1991). Temperature is linked to elevation, with a yearly average of 18 °C at 1800 m and 9 °C at 3000 m. Diurnal temperature swings of 11–16 °C represent the largest thermal variation (Schmitt, 1991).

The Aberdares' main habitat types include closed-canopy forest, heathland, high altitude grassland, and bare rock (Schmitt, 1991). The Aberdares range hosts large wildlife populations, particularly buffalo (*Syncerus caffer*), elephant (*Loxodonta africana*), and hyena (*Crocuta crocuta*). Bongo are found primarily within the ~1120 km<sup>2</sup> forest zone, and avoid the higher, non-forested habitats (Kingdon, 1982). Lower forests are dominated by coniferous *Podocarpus* and *Juniperus* species in drier habitats, and the flowering hardwoods *Cassipourea*, *Neoboutonia*, *Macaranga*, and *Olea* in more humid locations. Extensive, near monotypic stands of bamboo are found between 2500–3000 m, and the narrow belt of forest above this (~3000–3300 m) is dominated by *Hagenia abyssinica*, which gives way to heath and grassland (Schmitt 1991). Lower forest margins are defined by protected area boundaries at ~2000 m, below which lie dense rural settlements.

The Aberdares are protected as a national park above 3000 m and in an eastern spur that extends down to 2100 m, with the remaining area between the national park boundaries and human settlements designated as forest reserve (KWS, 2006; Lambrechts et al., 2003). A project to fence the Aberdare National Park and parts of the forest reserve has enclosed all but ~65 km along the Aberdares western escarpment (Rhino-Ark, 2006). This study focuses on the Aberdares' forests, excluding those lying outside the fence (Fig. 1C).

#### 2.1.2. Background on bongo ecology

Most of the information on bongo ecology is found in studies of the lowland bongo (Elkan 2003; Hillman & Gwynne, 1987; Klaus et al., 1998; Klaus-Hugi et al., 2000; Turkalo & Klaus-Hugi, 1999), which occurs in Central and West Africa. The lowland bongo's gregariousness sets it apart from other, typically solitary, forest ungulates (Estes, 1974; Klaus-Hugi et al., 1999). Herds of female and young may aggregate into concentrations of 50 or more animals, although males are more solitary, wider-ranging, and non-territorial (Estes, 1991; Hillman, 1986; Klaus-Hugi et al., 1999). Lowland bongo habitat is a mosaic of mineral-rich forest glades, secondary forest, and mature forest (Klaus-Hugi et al., 1999; Klaus-Hugi et al., 2000). Home ranges are organized around glades, which provide crucial mineral supplements and grasses that account for up to 30% of a lowland bongo's intake (Hillman & Gwynne, 1987; Klaus et al., 1998; Klaus-Hugi et al., 1999; Klaus-Hugi et al., 2000). Secondary forest provides cover and the browse (primarily tall forbs, understory shrubs, and lianes) that forms the majority of the animal's diet (Klaus-Hugi et al., 1999). Mature forest constitutes a less-utilized matrix, as its structure inhibits the growth of typical bongo food plants (Klaus-Hugi et al., 1999).

The mountain bongo shares the same social characteristics and an apparent preference for secondary forests and glade habitats (Kingdon, 1982). However, lowland and montane forests are substantially different, as the latter are characterized

by extensive stands of bamboo (*Sinarundinaria alpine*) and an altitudinal stratification of vegetation types (Schmitt, 1991; Bussmann, 1994). The bongo is believed to migrate along the elevation gradient as seasons change (Kingdon, 1982). These factors indicate that mountain bongo habitat is configured differently than the lowland bongo's.

## 2.2. Data

### 2.2.1. Remotely-sensed data

We used four RS datasets in this study: 1) two 5 m resolution SPOT 5 panchromatic scenes, acquired on February 17, 2006 (source: Terra Image USA [www.terraimageusa.com](http://www.terraimageusa.com)); 2) the three visual/near infrared (VNIR) bands (0.52–0.86  $\mu\text{m}$ , 15 m resolution) and six shortwave infrared (SWIR) bands (1.60–2.43  $\mu\text{m}$ , 30 m resolution) of two ASTER L1A scenes collected on March 29, 2005; 3) a MODIS surface reflectance image from March 29, 2005 (463 m); 4) a 927 m MODIS nadir BRDF-adjusted 16-day reflectance image from March 22, 2005. Each MODIS image consisted of seven bands ranging from 0.46–2.16  $\mu\text{m}$ . ASTER and MODIS data were provided by the US Geological Survey ([edcimswww.cr.usgs.gov/pub/imswelcome/](http://edcimswww.cr.usgs.gov/pub/imswelcome/)). A 90 m resolution SRTM (version 2) digital elevation model (DEM) was also acquired (source: CGIAR [srtm.csi.cgiar.org](http://srtm.csi.cgiar.org)).

SPOT and ASTER images were ortho-rectified to remove significant geometric distortions caused by the rugged topography. Accuracy was assessed using GPS-acquired control points (3–5 m precision) and an independently ortho-rectified Landsat 7 ETM+ scene (source: Global Land Cover Facility, [www.landcover.org](http://www.landcover.org)) with sub-50 m precision (Tucker et al., 2004). The root mean square error (RMSE) between the corrected SPOT data and control points was less than 10 m, while the RMSE between matched ASTER and SPOT image features was 7 m. Both image sets were more precise than the Landsat scene. MODIS images were not ortho-rectified.

We converted the ASTER images from at-sensor radiance to top of atmosphere reflectance using available conversion coefficients (Smith, 2006), and used dark-target subtraction to remove atmospheric effects (Jensen, 1996). The SPOT imagery was left in digital number format and did not require atmospheric correction, because the subsequent analytical technique (texture analysis) is insensitive to atmospheric effects. The MODIS data were already atmospherically corrected, although it was necessary to remove striping in two bands of the 463 m image using Fourier transform filters, which corrected most of this error. Minor cloud cover was manually digitized and masked out of the SPOT, ASTER, and MODIS 463 m data.

All data required topographic correction to remove terrain shadows. The SCS+C correction was applied to SPOT and ASTER scenes (Soenen et al., 2005), while the SCS correction (Gu & Gillespie, 1998) was used for MODIS images. Both corrections normalize reflectance ( $L$ ) by adjusting for slope ( $\alpha$ ), the solar zenith angle, and the solar incidence angle ( $i$ ). The SCS+C correction differs in that it includes a term (derived from a regression of  $i$  and  $L$ ) to account for the poor performance of SCS when  $\alpha$  is extreme (Soenen et al., 2005). The DEM aggregated to MODIS

scales did not produce high  $\alpha$  values. To provide  $\alpha$  for SPOT and ASTER images, the 90 m DEM was re-sampled to 5, 15, and 30 m resolution using a splining function.

The off-nadir look angles of the ASTER, SPOT, and 463 m MODIS scenes required the following adjustment to  $\alpha$ :

$$\alpha_{\text{adj}} = \alpha - \sin(\gamma - \varphi)\omega. \quad (1)$$

Where:  $\alpha_{\text{adj}}$  is adjusted slope,  $\gamma$  is terrain aspect,  $\varphi$  is the sensor track azimuth, and  $\omega$  is the sensor look angle (positive for right of nadir on a descending orbit, and negative for left). An author of the SCS+C correction confirmed the modification's validity (Coburn, Pers. Comm., 2006).

### 2.2.2. Field data

We collected field data over three periods representative of the Aberdares climate: the cool, misty long dry season (June–August, 2005), the hot, short dry season (February–March, 2006), and the end of the long rains (May–June, 2006). Field work was conducted with experienced trackers from the local Bongo Surveillance Program and Kenya Wildlife Service rangers (the park authority). Over the course of 12 expeditions covering 92 days, forests were surveyed for bongo tracks, dung and other signs that indicated habitat use (e.g. feeding, lying). A “reconnaissance” approach was used, where a general heading was maintained while following paths of least resistance (Walsh & White, 1999). Plots of 22.6 m diameter (the nominal diameter of 1/25 ha circular plots) were centered on bongo habitat-use sign that could be confidently identified. Following James and Shugart (1970), the following variables were recorded: diameter at breast height (DBH) of trees larger than 7.5 cm; top height of the three highest trees (using a clinometer); the number and species of breast-height shrubs (<7.5 cm DBH) and herbaceous plants (forbs) within two 22.6  $\times$  1.2 m transects; canopy and ground cover proportions (based on 20 readings for each); the average herbaceous layer height (20 readings). The same habitat data were recorded at pre-assigned plots centered in 1 km<sup>2</sup> grid cells laid over the study area. These points, representing bongo absence, were sampled if surveys passed within 200 m and no bongo sign were found. Plots were located and geo-referenced using a global positioning system (GPS) with an antenna. Error caused by dense canopy and steep terrain was reduced by raising the antenna on a 5 m pole and averaging positional fixes for 30–120 min.

We collected 150 field plots, eight of which were recorded using a variable plot method; these were reconciled to the fixed plots using photo-interpretation. The total count included 36 plots where bongo were indicated, 90 non-bongo plots (Fig. 1C), and 24 plots with waterbuck *Kobus ellipsiprymnus* sign. The waterbuck plots were used only to assess correlations between field and RS variables. The identity of the 36 bongo plots was confirmed using mitochondrial DNA extracted from dung specimens within or in the vicinity of sample plots. The waterbuck plots were initially thought to be bongo-use sites but were eliminated by mitochondrial DNA evidence. Hence, these plots were included in a calibration data set but eliminated from any formal analysis of bongo habitat selection.

Table 1  
The origin, derivation techniques, names, resolutions (res), scales, units, subsequent transformations, and basic statistics<sup>1</sup> (segregated according to bongo presence and absence) of the 60 RS and field data variables

Dataset	Derivation technique <sup>3</sup>	Variable name <sup>4</sup>	Res (m)	Scale (ha)	Units <sup>5</sup>	Transformed <sup>6</sup>	Bongo <i>n</i> =34, 36 <sup>2</sup>			Non-bongo <i>n</i> =83, 90 <sup>2</sup>		
							Mean	SD	Range	Mean	SD	Range
ASTER bands 1–9	SMA	GREENVEG	30	0.09	–	PCA 1	<b>0.32*</b>	0.10	0.16–0.57	<b>0.37*</b>	0.10	0.09–0.65
	SMA	NPVEG	30	0.09	–	PCA 1	0.06	0.02	0.01–0.14	0.07	0.04	0.02–0.29
	SMA	SOIL	30	0.09	–	PCA 1	0.06	0.02	0.01–0.12	0.07	0.03	0.02–0.17
	SMA	SHADE	30	0.09	–	PCA 1	<b>0.56**</b>	0.11	0.30–0.74	<b>0.49**</b>	0.09	0.28–0.69
	Aggregation of SMA fractions	GREENVEG	105	1.10	–	PCA 1	<b>0.33*</b>	0.08	0.18–0.48	<b>0.37*</b>	0.08	0.11–0.54
	Aggregation of SMA fractions	NPVEG	105	1.10	–	PCA 1	<b>0.06*</b>	0.01	0.04–0.09	<b>0.07*</b>	0.02	0.02–0.18
	Aggregation of SMA fractions	SOIL	105	1.10	–	PCA 1	<b>0.06**</b>	0.02	0.02–0.11	<b>0.07**</b>	0.02	0.03–0.16
	Aggregation of SMA fractions	GREENVEG	225	5.06	–	PCA 1	<b>0.33*</b>	0.07	0.20–0.48	<b>0.37*</b>	0.08	0.10–0.53
	Aggregation of SMA fractions	NPVEG	225	5.06	–	PCA 1	<b>0.06***</b>	0.01	0.04–0.10	<b>0.07***</b>	0.02	0.03–0.16
	Aggregation of SMA fractions	SOIL	225	5.06	–	PCA 1	<b>0.06*</b>	0.02	0.03–0.11	<b>0.07*</b>	0.02	0.03–0.15
	Aggregation of SMA fractions	GREENVEG	450	20.25	–	PCA 1	<b>0.34*</b>	0.05	0.23–0.46	<b>0.37*</b>	0.08	0.11–0.52
	Aggregation of SMA fractions	NPVEG	450	20.25	–	PCA 1	<b>0.05****</b>	0.01	0.04–0.07	<b>0.07****</b>	0.02	0.03–0.12
	Aggregation of SMA fractions	SOIL	450	20.25	–	PCA 1	<b>0.06***</b>	0.01	0.04–0.09	<b>0.07**</b>	0.02	0.04–0.15
	ASTER band 1	Mean TF 3×3	3×3 B1M	15	0.20	1	PCA 2	<b>284.49**</b>	49.44	199.12–419.09	<b>316.40**</b>	67.92
Standard deviation TF 3×3		3×3 B1SD	15	0.20	1	PCA 2	28.23	13.92	6.36–78.38	25.06	14.64	7.71–80.48
Angular second moment TF 3×3		3×3 B1ASM	15	0.20	–	PCA 2	<b>1.00*</b>	0.00	1.00–1.00	<b>0.95*</b>	0.15	0.26–1.00
ASTER band 2	Mean TF 3×3	3×3 B2M	15	0.20	1	PCA 2	<b>236.49**</b>	47.53	158.46–373.91	<b>272.26**</b>	81.57	161.90–775.13
	Standard deviation TF 3×3	3×3 B2SD	15	0.20	1	PCA 2	24.68	10.88	10.11–51.20	26.61	19.40	6.40–114.57
	Angular second moment TF 3×3	3×3 B2ASM	15	0.20	–	PCA 2	0.69	0.27	0.26–1.00	0.68	0.27	0.26–1.00
ASTER band 3	Mean TF 3×3	3×3 B3M	15	0.20	1	PCA 2	<b>1663.52**</b>	387.70	1008.19–2720.41	<b>1888.74**</b>	374.74	884.33–2787.44
	Standard deviation TF 3×3	3×3 B3SD	15	0.20	1	PCA 2	179.32	94.45	31.42–535.74	153.25	71.89	32.64–315.56
	Angular second moment TF 3×3	3×3 B3ASM	15	0.20	–	PCA 2	0.79	0.26	0.28–1.00	0.85	0.24	0.28–1.00
ASTER band 1	Mean TF 7×7	7×7 B1M	15	1.10	1	PCA 2	<b>284.83**</b>	41.72	198.97–386.53	<b>315.88**</b>	55.55	210.25–601.84
	Standard deviation TF 7×7	7×7 B1SD	15	1.10	1	PCA 2	36.61	13.70	13.45–67.42	37.00	19.46	14.86–119.08
	Angular second moment TF 7×7	7×7 B1ASM	15	1.10	–	PCA 2	<b>1.00**</b>	0.00	1.00–1.00	<b>0.94**</b>	0.13	0.44–1.00
ASTER band 2	Mean TF 7×7	7×7 B2M	15	1.10	1	PCA 2	<b>237.67**</b>	41.23	155.41–340.72	<b>270.22**</b>	63.90	157.16–642.10
	Standard deviation TF 7×7	7×7 B2SD	15	1.10	1	PCA 2	33.83	13.01	13.71–64.72	39.49	27.34	10.15–172.86
	Angular second moment TF 7×7	7×7 B2ASM	15	1.10	–	PCA 2	0.57	0.28	0.25–1.00	0.59	0.26	0.16–1.00
ASTER band 3	Mean TF 7×7	7×7 B3M	15	1.10	1	PCA 2	<b>1699.67**</b>	354.46	1055.95–2511.19	<b>1894.97**</b>	348.91	914.95–2670.47
	Standard deviation TF 7×7	7×7 B3SD	15	1.10	1	PCA 2	232.45	99.40	76.89–422.16	207.66	77.83	60.45–462.64
	Angular second moment TF 7×7	7×7 B3ASM	15	1.10	–	PCA 2	0.78	0.25	0.26–1.00	0.80	0.25	0.27–1.00
MODIS daily surface reflectance	SMA	GREENVEG	463	21.44	–	PCA 1	<b>0.33***</b>	0.05	0.24–0.44	<b>0.37***</b>	0.06	0.22–0.51
	SMA	NPVEG	463	21.44	–	PCA 1	0.02	0.02	0.00–0.08	0.02	0.02	–0.04–0.06
	SMA	SOIL	463	21.44	–	PCA 1	0.07	0.06	–0.01–0.22	0.06	0.05	–0.03–0.27
	SMA	SHADE	463	21.44	–	PCA 1	<b>0.58*</b>	0.06	0.44–0.68	<b>0.56*</b>	0.04	0.41–0.68
MODIS BRDF Nadir-adjusted reflectance	SMA	GREENVEG	927	85.93	–	PCA 1	<b>0.38*</b>	0.05	0.26–0.45	<b>0.41*</b>	0.06	0.24–0.54
	SMA	NPVEG	927	85.93	–	PCA 1	0.03	0.01	0.01–0.07	0.03	0.02	0.00–0.10
	SMA	SOIL	927	85.93	–	PCA 1	0.05	0.02	–0.01–0.11	0.06	0.04	–0.01–0.17
	SMA	SHADE	927	85.93	–	PCA 1	<b>0.54****</b>	0.06	0.46–0.67	<b>0.50****</b>	0.05	0.43–0.65

SPOT panchromatic	Mean TF 3×3	3×3 M	5	0.02	DN	PCA 3	7316.32	748.86	5918.00–10154.00	7681.94	1112.56	5959.00–13490.00	
	Standard deviation TF 3×3	3×3 SD	5	0.02	DN	PCA 3	490.38	224.67	129.00–1169.00	408.06	262.18	106.00–1406.00	
	Angular second moment TF 3×3	3×3 ASM	5	0.02	DN	PCA 3	<b>0.17*</b>	0.06	0.11–0.38	<b>0.22*</b>	0.11	0.11–0.63	
	Mean TF 5×5	5×5 M	5	0.06	DN	PCA 4	7321.35	681.64	6102.00–9850.00	7697.41	1055.84	5975.00–13399.00	
	Standard deviation TF 5×5	5×5 SD	5	0.06	DN	PCA 4	<b>579.24*</b>	212.77	143.00–1137.00	<b>505.69*</b>	327.09	145.00–1729.00	
	Angular second moment TF 5×5	5×5 ASM	5	0.06	DN	PCA 4	<b>0.10*</b>	0.06	0.06–0.36	<b>0.14*</b>	0.08	0.05–0.35	
	Mean TF 9×9	9×9 M	5	0.20	DN	PCA 4	<b>7284.50*</b>	582.94	6307.00–9093.00	<b>7703.31*</b>	995.44	6015.00–13465.00	
	Standard deviation TF 9×9	9×9 SD	5	0.20	DN	PCA 4	677.50	254.27	206.00–1497.00	581.45	335.53	212.00–1795.00	
	Angular second moment TF 9×9	9×9 ASM	5	0.20	DN	PCA 4	<b>0.07*</b>	0.05	0.03–0.27	<b>0.10*</b>	0.07	0.03–0.38	
	Mean TF 21×21	21×21 M	5	1.10	DN	PCA 4	<b>7298.68**</b>	498.50	6330.00–8617.00	<b>7692.92**</b>	812.92	6408.00–12370.00	
	Standard deviation TF 21×21	21×21 SD	5	1.10	DN	PCA 4	744.15	237.45	268.00–1289.00	722.12	396.63	240.00–2397.00	
	Angular second moment TF	21×21 ASM	5	1.10	DN	PCA 4	<b>0.05*</b>	0.05	0.01–0.30	<b>0.07*</b>	0.05	0.01–0.25	
	Field data	1	Basal Area <sup>a</sup>	22.6	0.04	m <sup>2</sup> ha <sup>-1</sup>	–	<b>39.45****</b>	37.50	0.00–141.36	<b>16.80****</b>	21.28	0.00–98.04
		2	Stem density <sup>a</sup>	22.6	0.04	n ha <sup>-1</sup>	–	297.06	301.35	0.00–1171.63	232.66	281.04	0.00–1096.85
3		Canopy height <sup>a</sup>	22.6	0.04	m	–	<b>17.36**</b>	9.09	1.55–42.41	<b>12.13**</b>	6.17	0.90–26.10	
4		Canopy cover <sup>a</sup>	22.6	0.04	–	–	0.80	0.25	0.00–1.00	0.73	0.29	0.00–1.00	
2		Bamboo density <sup>a</sup>	22.6	0.04	n ha <sup>-1</sup>	–	13874.10	22828.02	0.00–110687.9	9186.36	15493.33	0.00–72932.51	
2		Shrub density <sup>b</sup>	22.6	0.04	n ha <sup>-1</sup>	–	<b>1474.36*</b>	1819.39	0.00–7366.92	<b>4308.43*</b>	5215.52	0.00–24815.91	
2		Tall forb density <sup>b</sup>	22.6	0.04	n ha <sup>-1</sup>	–	<b>6178.03*</b>	5861.21	133.72–20259.03	<b>3494.03*</b>	4112.13	0.00–23266.51	
4		Ground cover <sup>b</sup>	22.6	0.04	–	–	0.83	0.14	0.35–1.00	0.78	0.18	0.10–1.00	
4	Herbaceous height <sup>b</sup>	22.6	0.04	–	–	3.10	0.82	1.00–4.70	2.86	0.99	0.90–5.70		

<sup>1</sup>Significantly different means are indicated in boldface, with asterisks denoting alpha level (\*:  $p < 0.05$ ; \*\*:  $p < 0.01$ ; \*\*\*:  $p < 0.001$ ; \*\*\*\*:  $p < 0.0001$ ).

<sup>2</sup>Total number of plots varies by data type. The first value indicates the number of field plot localities that were not obscured by cloud cover (34 bongo and 83 non-bongo) that could be used to extract RS-derived variables. The second refers to the number of available presence/absence field data plots (36 bongo and 90 non-bongo).

<sup>3</sup>Key to derivation techniques: SMA — Spectral mixture analysis; Aggregation of SMA fractions — Obtained by averaging the 30 m SMA endmember fractions, excluding the SHADE fraction because it is a linear combination of the other fractions, which prevents the unique solution required for logistic regression models; TF — Texture filter; 3×3, 5×5, 7×7, 9×9, 21×21 — The window sizes used in texture analysis; 1 — Plot basal area =  $\sum(n \text{ trees per } 5 \text{ cm DBH class} \times (II \text{ (DBH/200)}^2))$ ; 2 — Plot stem density =  $\sum(n \text{ trees per } 5 \text{ cm DBH class per plot} \times (10,000 \text{ m}^2/\text{Plot area}))$ . Other plot density measures =  $n$  (shrubs, tall forbs, or bamboo)  $\times (10,000 \text{ m}^2/\text{Area of plot strip transects})$ ; 3 — Plot canopy height = mean height of the 3 tallest trees/shrubs; 4 — Cover variables are the proportion of plant to non-plant cover taken from 20 readings; 5 — Herbaceous height = the mean of 20 height measurements based on 7 different height classes.

<sup>4</sup>Variable name: GREENVEG — the green vegetation endmember fraction; NPVEG — the nonphotosynthetic vegetation endmember fraction; SOIL — the soil endmember fraction; SHADE — the SHADE endmember fraction; <sup>a</sup>Canopy structure variable; <sup>b</sup>Understorey structure variable.

<sup>5</sup>Key to units: 1 = Reflectance  $\times 10,000$ ; DN = digital numbers  $\times 1000$ .

<sup>6</sup>Refers to subsequent transformations of the variables sets. Principal components analysis (PCA) was performed on each RS variable set representing a unique sensor-scale combination in order to 1) orthogonalize the data, and 2) to reduce the number of variables for subsequent logistic regression analyses (provided that at least 90% of explained variance could be retained): PCA 1 = the GREENVEG, NPVEG, and SOIL fractions of each SMA dataset were PC transformed — all three PCs were retained to account for 90% of variance; PCA 2 = The values of the 3 texture measures for all 3 ASTER VNIR bands were PC transformed (separated by window size), with PCs 1–5 retained; PCA 3 = The three 3×3 SPOT texture measures were PC transformed, with all three PCs retained; PCA 4 = the first two PCs of each set of the transformed 5×5, 9×9, and 21×21 SPOT texture measures were retained.

In a study of radio-collared White-tailed deer *Odocoileus virginianus*, Dunn (1978) found that positional observations were effectively uncorrelated after an average of 13.5 hours (min 7.9, max 22.6). In this study, the times at which neighboring pairs of bongo habitat use signs were made differed by an average of 57 days (range: ~24 hours–284 days). Although neighboring habitat use signs were closely-spaced (mean nearest neighbor distance=715.3 m), their temporal separation is sufficient for their corresponding data plots to be considered independent under Dunn's criteria. The trial removal of several samples with the least temporal separation during the subsequent logistic regression analyses (see Section 2.4 and following) showed that results were not altered appreciably.

### 2.3. Derived variables

We derived a total of 60 variables from the field and remotely-sensed data, ranging in spatial scale from 0.02–85.93 ha. Table 1 provides a list of these variables, including their derivation techniques, spatial scales, units of measure, and relevant transformations. Differences between mean variable values in bongo and non-bongo plots were assessed using a two-sided Wilcoxon rank-sum test, a non-parametric equivalent of the *t*-test used because most variables were non-normally distributed. Descriptions of the methodologies used to derive these variables follow in Sections 2.3.1–2.3.2.

#### 2.3.1. Remotely-sensed variables

We used two techniques to derive variables from the remotely-sensed data: spectral mixture and texture analysis. Spectral mixture analysis is a linear modeling technique that estimates the fractional abundance of specified constituents (endmembers) within a pixel using their spectral profiles (Adams et al., 1989). This technique is particularly useful for ascribing physical meaning to RS data, since it establishes a direct and easily interpretable link between the signal received by the sensor and the surface features shaping it (Sabol et al., 2002). Although designed for hyperspectral imagery, spectral mixture analysis is also applicable to multispectral data (e.g. Lu et al., 2003; Sabol et al., 2002). In texture analysis, information is obtained by measuring the spatial variation in an image's tonal values (Baraldi & Parmiggiani, 1995). Texture analysis of optical RS has been successfully used to quantify forest structural properties (Kayitakire et al., 2006; Wulder et al., 1998) and the spatial arrangement of species' habitats (St-Louis et al., 2006).

**2.3.1.1. Spectral mixture analysis.** We chose four endmembers useful for discriminating forest structure for the spectral mixture analysis: green vegetation (GREENVEG), nonphotosynthetic vegetation (NPVEG), soil (SOIL) and shade (SHADE) (Sabol et al., 2002; Lu et al., 2003). The endmembers were selected from available spectral libraries (ENVI, 2006) and averaged, then compared to the spectra of representative pixels located in known image features or in reflectance scatter-plots for similarity of shape and magnitude. Photometric (spectrally flat) shade was used for the endmember SHADE (following Roberts et al., 1998), thus the mixture model was unconstrained. Fractional endmembers result-

ing from unconstrained spectral mixture analysis can be negative or greater than one, which generally indicates a poor model fit (Roberts et al., 1998). Roberts et al. (1998) allowed endmember fractions to vary between 1.01 and -0.01, provided that all endmembers sum to one. For this analysis, we tolerated endmember fractions between -0.05 and 1.05 to accommodate topographically-induced errors and the lack of site-specific reference spectra. We applied spectral mixture analysis to the ASTER and two MODIS images. The final model for each sensor was selected if: 1) >99% of RMS values were below 0.03; 2) >99% of fractional values for each endmember were between -0.05 and 1.05.

**2.3.1.2. Texture analysis.** Image texture measures can be classified into two groups: 1) occurrence, which relates to the frequency of tonal values in a specified neighborhood around each pixel (St-Louis et al., 2006); 2) co-occurrence, which measures the frequency of associations between brightness value pairs within a given area (Baraldi & Parmiggiani, 1995). We applied two occurrence measures (mean and standard deviation) and one co-occurrence measure, angular second moment, to the SPOT image and the three ASTER VNIR bands. Mean and standard deviation are simple and useful for discriminating different habitat structures (St-Louis et al., 2006) or forest biophysical properties (Wulder et al., 1998). We selected angular second moment (which describes image textural uniformity) because it is uncorrelated with standard deviation and is one of the most informative co-occurrence measures (Baraldi & Parmiggiani, 1995).

**2.3.1.3. Scaling and transformation.** In their native 30 m resolution, the ASTER spectral mixture analysis endmember fractions are of similar scale to the field data plots. These ASTER variables were further aggregated to three coarser resolutions (Table 1). The 105 m resolution allowed comparison between spectral mixture analysis and the largest-scaled texture analyses, while the 450 m pixel size was selected to compare ASTER and MODIS at similar resolutions. The 225 m aggregation provided an intermediate scale between the two previous forest patch-sized aggregations. Texture analyses were performed on the SPOT image using four window sizes (Table 1). The first two window sizes bracket the field plot scale, while the two largest are equivalent in scale to the window sizes applied to the ASTER VNIR bands.

The number of RS-derived variables was large in relation to our sample size, and a number of RS measures were strongly correlated with one another. We therefore applied principal components analysis (PCA) to each set of variables representing a unique sensor-scale combination (e.g. 30 m ASTER end-member fractions). The SHADE fraction was dropped from each spectral mixture analysis variable set because it is a linear combination of the other three endmember fractions. We retained the principal components (PCs) accounting for at least 90% of total variance. PCA allowed us to maximize degrees of freedom (by decreasing the number of parameters) and reduce inter-variable correlations (and thus minimize variance inflation) while retaining the essential information in the RS variables used as predictors in subsequent logistic regression analyses (described in Section 2.4.2).

### 2.3.2. Micro-scale vegetation structure

We derived nine measures of micro-scale vegetation structure from the field data: five measures of canopy structure, and four of understorey structure (Table 1). Apart from bamboo density—an important vegetation type in the Aberdares—we chose these measures because: 1) they account for the range of structural types found in Aberdares forests, 2) they appear in previous RS studies of forest structure (e.g. Hansen et al., 2001; Lu et al., 2004; Peddle et al., 2004) or investigations of similar large herbivores (e.g. Terry et al., 2000), or 3) they describe the range of potential variation in cover and forage.

## 2.4. Statistical analysis

### 2.4.1. Remote detection of microhabitat structure

The first portion of our analysis followed Jeganathan et al.'s (2004) “two-step procedure” for modeling rare species' distributions. This approach entails 1) identifying the most important microhabitat variables by modeling the species' relationship with field-collected habitat data, and 2) relating these directly to RS data to generate physically meaningful, spatially extensive habitat variables.

For the first step, we used logistic regression to determine the field variables most likely to influence bongo habitat selection at the plot scale. Logistic regression, a form of the generalized linear model that applies the logit transformation to account for binomial error distribution in a categorical response variable (Trexler & Travis, 1993), was most appropriate given that our field plots were segregated according to bongo presence or absence (Table 1). The most likely set of bongo habitat predictors was selected using Akaike's Information Criterion modified for small sample sizes ( $AIC_c$ ):

$$AIC_c = -2\log L + 2K \left( \frac{n}{n - K - 1} \right). \quad (2)$$

Where:  $L$  is a model's likelihood,  $K$  is the number of parameters, and  $n$  is sample size (Burnham & Anderson, 2002). This information theoretic method yields more objective, consistent models than conventional hypothesis testing techniques (e.g. stepwise regression) by minimizing bias and maximizing precision (Burnham & Anderson, 2002).  $AIC_c$  is a relative measure, and is useful for comparing a pre-specified set of candidate models drawn from a common global model (Burnham & Anderson, 2002). The best fitting model is that which has the lowest  $AIC_c$  value, and its relative plausibility is assessed with the associated measures  $\Delta_i$  and  $w_i$ , the Akaike difference and weight (Burnham & Anderson, 2002). The former measures the difference between the  $AIC_c$  of model  $i$  and the best model, and can be interpreted as follows: the most likely model, given the data, has a  $\Delta_i$  of zero, values between 0 and 2 indicate strong support for a model, values between 4 and 7 show that a model has far less support, while models with values of 10 or higher are extremely unlikely (Burnham & Anderson, 2002). The Akaike weight is inversely proportioned to  $\Delta_i$ , and expresses the odds (as a ratio) that a given model is the best of the candidate set of models, given the data (Burnham & Anderson, 2002).

We selected candidate models representing likely combinations of canopy and understorey structure variables from the 10 parameter (including the regression intercept) global model, the fit of which was assessed using the Hosmer–Lemeshow test (Hosmer & Lemeshow, 1989). This measure partitions observations into equally sized groups, and compares differences in observed and expected values against the  $\chi^2$  distribution—an acceptance of the null hypothesis indicates an adequate fit. An additional pseudo  $r^2$  measure was included with the information theoretic statistics to provide a more understandable metric of variance explained by the predictors—not as a basis for model selection. This measure, the adjusted sum of squares  $R^2$  ( $R_{SS,adj}^2$ ), is described by Mittlbock and Schemper (1999), and is analogous to the  $R^2$  of least squares regression.

In the second step, we used Spearman rank correlation analysis to assess the relationship between RS-derived measures and the most influential field-based microhabitat variables in order to determine 1) how well RS data can detect the microhabitat variables most correlated with bongo presence, and 2) the physical meaning of each RS variable. We applied the sequential Bonferroni adjustment (Holm, 1979) to reduce the likelihood of spurious significant correlations using the following procedure: the  $p$ -values resulting from each RS-field predictor comparison (segregated by sensor type) were ordered from most significant to least; the  $p$ -value of the most significant pairing was adjusted ( $p_{adj} = 0.05/n$ , where  $n$  = variables per sensor \* field variables); successive pairings were assessed against  $p < 0.05/(n-1)$ ,  $p < 0.05/(n-2)$ ,  $p < 0.05/(n-3)$ , etc., until a comparison failed to reject the null hypothesis. We utilized all 150 field data points for this portion of the analysis, excluding one ASTER, two SPOT, and three MODIS points falling within cloud-shadowed areas.

### 2.4.2. Multi-scaled modeling of bongo habitat selection

Using the logistic regression and model selection methods specified in Section 2.4.1, we assessed the relative abilities of the different datasets and their associated scales to explain bongo habitat selection. This analysis was undertaken in two parts. In the first part, we tested the ability of each set of PCA-transformed variables representing a unique sensor-scale combination to predict bongo habitat selection. Our primary aim was to reduce the large number of RS variables for the second part, in which we combined the resulting three most likely RS variable sets with the most important field-derived microhabitat predictors identified in the analysis described in Section 2.4.1. This final analysis allowed us to assess 1) the habitat features and spatial scales most influencing bongo habitat selection, and 2) the relative explanatory power of the best field and RS predictors.

## 3. Results

### 3.1. Derived RS variables

For the spectral mixture analysis performed on the three image-sets, the resulting root mean squared errors (RMS), RMS

standard deviations, and percentages of pixels falling outside the endmember fraction threshold of  $-0.05$  and  $1.05$  for the best models were:  $0.009$ ,  $0.003$ , and  $0.01\%$  (ASTER);  $0.014$ ,  $0.004$ , and  $0.36\%$  (MODIS 463 m);  $0.014$ ,  $0.0034$ , and  $0.16\%$  (MODIS 927 m). The ASTER endmember fractions produced sensible results when compared to known field conditions, as seen at sites 1, 2, and 3 in Fig. 2C–F. Site 1 is in mature, semi-open forest dominated by the tree *Hagenia abyssinica*, which has spreading crowns with large, bright green leaves creating abundant canopy shadows. A co-dominant shrub, *Hypericum revolutum*, occupies much of the understorey, and the herbaceous layer is well developed. Bright green vegetation is therefore a dominant feature in this forest type, while bare soil is generally not visible. The endmember fractions match this pattern: GREENVEG is high, NPVEG and SOIL are low, and SHADE is generally high. Site 2 is an open short grass glade, where the usually green rhizomatous grasses mix with tussock grasses that are composed of both live and senesced material. Animal activity and incomplete grass cover create abundant bare soil patches. The low SHADE, moderate GREENVEG, and high NPVEG and SOIL fractions appear reasonable given these conditions. Site 3 is in an area surrounded by extensive bamboo forest, which typically form

monotypic, dense canopies of uniform height ranging from 4–16 m. The perpetual shade under bamboo canopies tends to suppress understorey growth, while the ground is covered by bamboo leaf litter. The endmember patterns make sense for these conditions; GREENVEG is fairly high (bamboo appears as a uniform sea of green from above), NPVEG and SOIL are moderate to low (dead leaves and soil are abundant under bamboo, but are less evident from above because of the closed-canopy), and SHADE is high.

A total of 12 SPOT and 18 ASTER texture images were produced (Table 1). Fig. 2B is a sub-scene of the SPOT  $9 \times 9$  standard deviation image. Sites 4 and 5 were recorded in small forest openings, and thus have high standard deviations because of their close proximity to the much darker mature forest. Plots 1, 2, and 3 have low values because they are not close to the edges of their respective habitats.

### 3.2. Remote detection of microhabitat structure

The univariate statistics show that the means of four field-derived microhabitat measures were significantly different between bongo and non-bongo plots (Table 1). Of the canopy measures, basal area was significantly higher at bongo than non-

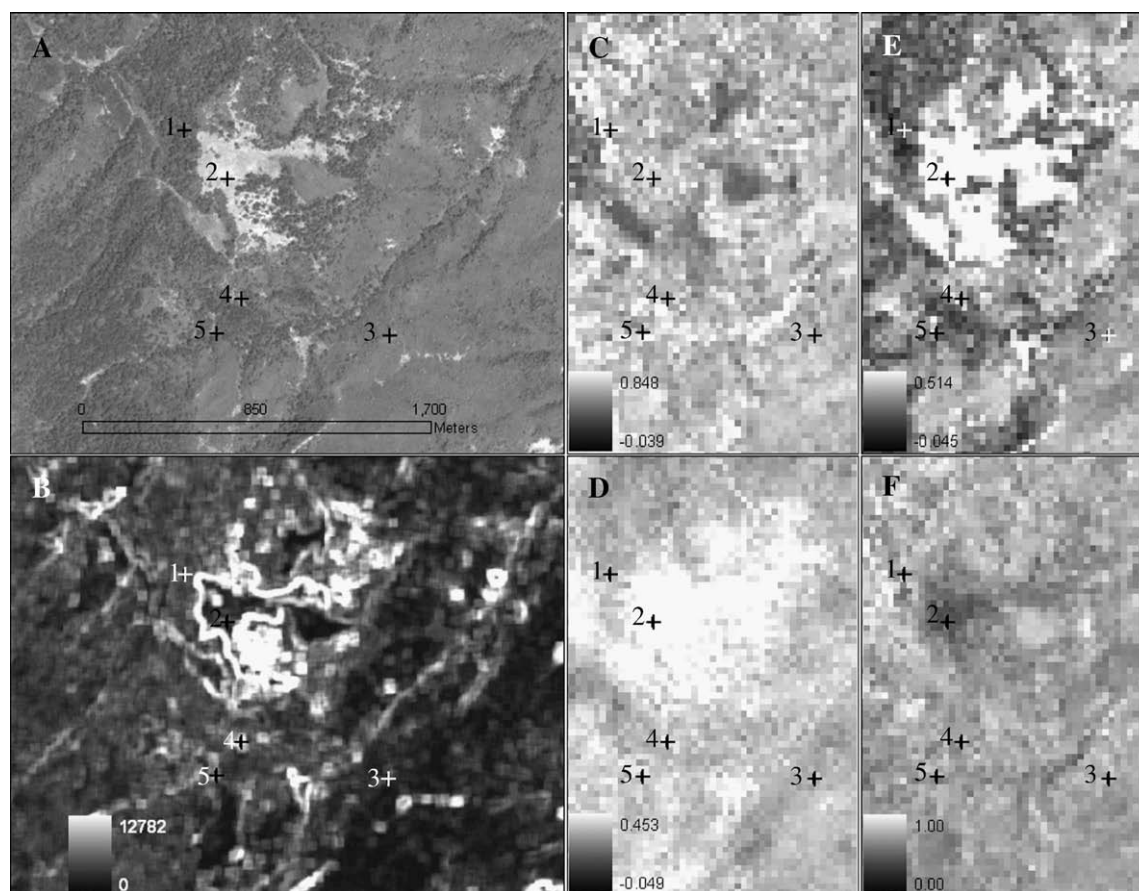


Fig. 2. Selected results of RS image analyses. A portion of the study area is illustrated by A) the SPOT 5 m panchromatic image, and B) the SPOT  $9 \times 9$  standard deviation texture image. The same area is shown in the four right-hand images, which are the C) GV, D) soil, E) NPV, and F) shade fractional endmembers resulting from SMA of the 30 m ASTER image. The numbered crosses indicate the locations of field sample plots: site 1 is located in mature, semi-open *Hagenia* forest; site 2 falls within a large short-grass glade; site 3 lies in bamboo forest; sites 4 and 5 are in small, partially shrubby clearings within a larger *Hagenia* forest.

bongo sites, as was canopy height. Among the understory variables, woody shrub density was significantly lower in bongo plots, while the density of tall forbs was significantly higher. This simple analysis indicating microhabitat selection set the stage for the more complex assessment of each variable's relative influence using logistic regression, in which we tested 27 models representing different combinations of the five canopy and four understory variables (ranging from four to nine parameters, including the intercept). Table 2 presents the information measures of the seven most likely models, the global model, and the highest ranked models employing canopy or understory variables only.

The results show that each of the top seven models has strong support for being the most likely given the data, as indicated by their sub-two  $\Delta$  values and similar  $w$  terms. Although this tight ranking indicates substantial model selection uncertainty (Burnham & Anderson, 2002), these models have two common features: basal area is present in all seven, as are at least three (and usually all four) of the understory measures. This suggests that basal area and the four understory variables are the fundamental measures for characterizing bongo habitat.

Of the remaining canopy measures, bamboo density and canopy cover may also be important predictors, as each appears three (canopy cover) or four (bamboo density) times in the top seven models, and once each in the first and second ranked models. Stem density possibly has influence, as it is found in models 5 and 7. Canopy height appears in none of the top models, and is therefore unimportant. Models based on understory or

canopy variables only are highly unlikely, given the low rankings and high  $\Delta$  values of the top performers for these model types.

We selected the four canopy and four understory variables from the top seven models for correlation analysis with the 42 RS variables (excluding the aggregated ASTER spectral mixture analysis endmember fractions). Fig. 3 provides a graphical display of the resulting correlation coefficients, excluding 10 RS variables (ASTER Band 2 and 3 angular second moment ( $3 \times 3$  and  $7 \times 7$ ); ASTER Band 3  $3 \times 3$  and  $7 \times 7$  SD; MODIS 463 and 927 NPVEG and SOIL fractions) that had no significant relationships with any microhabitat variables after sequential Bonferroni adjustment.

The general pattern of the results shows that the RS data correlate fairly well with canopy structure (with 60 of the 168 comparisons being significant) and rather poorly with understory structure (only two significant comparisons), as might be expected for optical RS data.

The RS data are most strongly related with basal area, with the ASTER and SPOT texture means producing the only seven correlations with absolute  $r$  values greater than 0.5. Canopy cover is the next most strongly correlated with RS variables, despite having 23 significant correlations with RS variables compared to basal area's 23. The SPOT  $3 \times 3$  and  $5 \times 5$  texture means were the best correlates of canopy cover ( $r = -0.49$ ), while ASTER texture measures were slightly weaker in their relationships with this variable. Stem density and bamboo density follow in decreasing order in terms of number of significant correlations with RS variables (15 and 5) and correlation strength (absolute maximum  $r = 0.45$  and  $0.42$ ).

Overall canopy structural variables were best detected by ASTER and SPOT texture measures (particularly mean texture) derived using the window sizes most closely matched in scale to that of field plot. The finer-resolution SPOT imagery produced slightly stronger correlations with canopy cover than ASTER, but the spectrally deeper ASTER succeeds where SPOT fails in correlating significantly with bamboo density (two texture variables and the GREENVEG fraction).

Correlations between the 30 m ASTER spectral mixture analysis endmember fractions and canopy structure were generally weaker than those found using texture measures derived from the 15 m ASTER VNIR and 5 m SPOT imagery. However, nine of the 16 (56%) comparisons between ASTER endmember fractions and canopy variables were significant, which compares favorably to the 32 and 42% significance rates achieved by ASTER and SPOT texture-canopy variable correlations, respectively. The coarse resolution MODIS SMA fractions showed the weakest relationships with canopy structure variables, with the strongest  $r$  being  $-0.36$ .

### 3.3. Multi-scaled modeling of bongo habitat selection

Having established the RS data's physical meaning by examining its relationships with microhabitat structure, the next step was to determine the features and scales that influence bongo habitat selection. To do this, we tested combinations of the most useful RS and field predictors of bongo habitat selection in multiple logistic regression models.

Table 2

Selected results of the multiple logistic regression models based on specified combinations of the field-collected microhabitat variables (canopy structure variables are presented in bold; understory variables in plain text)

Rank	Model ( $R=27$ , $n=126$ )*	$K^\dagger$	AIC <sub>c</sub>	$\Delta_i$	$w_i$	$R_{ss,adj}^2$
1	<b>BA, Bamb</b> , Shrub, Forb, HH	6	125.00	0.00	0.14	0.24
2	<b>BA, CC</b> , Shrub, Forb, HH	6	125.20	0.21	0.13	0.23
3	<b>BA</b> , Shrub, Forb, GC, HH	6	125.22	0.22	0.13	0.24
4	<b>BA, Bamb</b> , Shrub, Forb, GC, HH	7	125.42	0.42	0.12	0.24
5	<b>BA, SD</b> , CC, Bamb, Shrub, Forb, GC, HH	9	126.34	1.34	0.07	0.25
6	<b>BA, CC</b> , Shrub, Forb, GC, HH	7	126.89	1.89	0.06	0.23
7	<b>BA, SD, Bamb</b> , Shrub, Forb, GC, HH	8	126.92	1.93	0.06	0.25
<b>9</b>	<b>BA, SD, HGT, CC, Bamb</b> , Shrub, Forb, GC, HH <sup>‡</sup>	10	127.18	2.19	0.05	0.26
21	Shrub, Forb, GC	4	133.22	8.22	0.00	0.17
24	<b>BA, HGT, Bamb</b>	4	138.50	13.50	0.00	0.13

The results of the five best models, the best models using canopy and understory variables only, and the global model (denoted by the boldface, underlined model rank) are presented. Models were ranked and evaluated using the modified Akaike's Information Criterion (AIC<sub>c</sub>), the Akaike difference ( $\Delta_i$ ), and Akaike weights ( $w_i$ ). The adjusted sum of squares  $R^2$  ( $R_{ss,adj}^2$ ) indicates the proportion of variance explained in the response.

\* $R$ =number of candidate models, BA=basal area; SD=stem density; HGT=canopy height; CC=proportion canopy cover; Bamb=bamboo density; Shrub=shrub density; Forb=tall forb density; GC=proportion ground cover; HH=relative height of herbaceous layer.

<sup>†</sup> $K$ =number of predictors plus regression intercept.

<sup>‡</sup>Hosmer–Lemeshow test result:  $\chi^2=3.68$ ,  $df=8$ ,  $p<0.88$ .

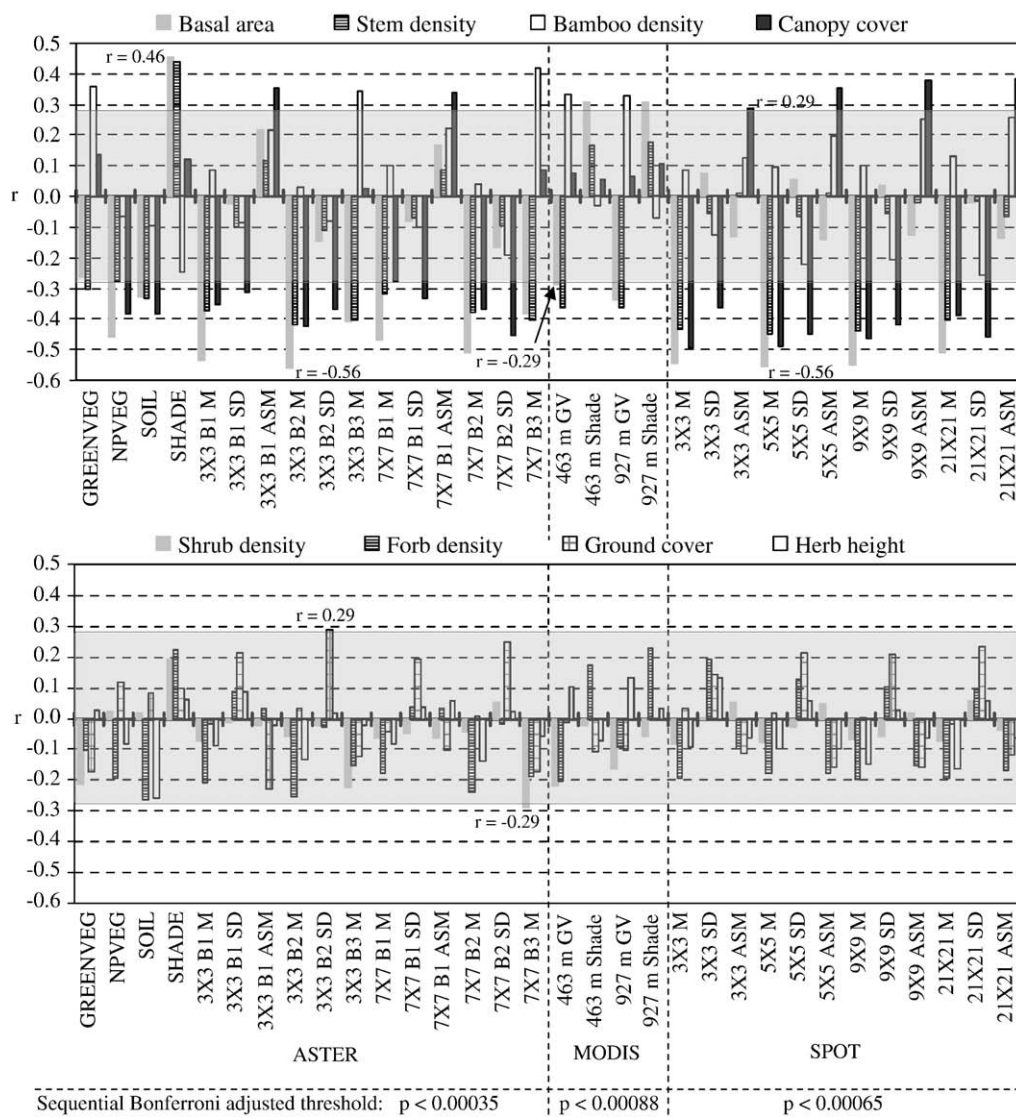


Fig. 3. A graphical presentation of Spearman Rank correlation coefficients, indicating the strength and direction of relationships between the RS and microhabitat variables. Coefficient bars are coded according to the microhabitat variable assessed; the upper graph contains canopy structure variables, while the lower graph contains understory variables. Bars extending outside the grey-shaded area are significant at the indicated sequential Bonferroni-adjusted alpha levels; those within the shaded area are not. RS variables appear on the X axes, and are segregated by sensor. SMA variables are denoted by their endmember fraction names (GREENVEG, NPVEG, SOIL, SHADE), while texture variables are listed according to window size and measure:  $M$ =mean;  $SD$ =standard deviation;  $ASM$ =angular second moment. Variables that showed no significant relationship with any microhabitat feature are not listed. These are: ASTER  $3 \times 3$  Band 2 ASM, Band 3 SD, Band 3 ASM; ASTER  $7 \times 7$  Band 2 ASM, Band 3 SD, Band 3 ASM; MODIS 463 m NPV and soil, MODIS 927 m NPV and soil.

We selected the most likely RS predictors of bongo habitat selection in a preliminary logistic regression analysis of PCA-transformed RS variable sets (see Table 1) representing unique sensor-scale combinations. This analysis (presented in Appendix A) showed that the PCs of the 450 m (20.25 ha) ASTER spectral mixture analysis endmember fractions were the most likely predictors of bongo habitat selection, as they provided the only two models with sub-two  $\Delta$  values. The next best predictors were provided by PCs of the 225 m (5.06 ha) ASTER endmember fractions, followed by PCs of the SPOT  $9 \times 9$  (0.2 ha) texture measures, although the  $\Delta$  values of the models created using both variable sets were greater than 10. All other variables, including MODIS endmember fractions and ASTER texture measures, were highly unlikely predictors.

Based on this finding, we combined the three 20.25 ha ASTER spectral mixture analysis PCs with the seven variables used in the three most likely microhabitat selection models (Table 2) for the final logistic regression analysis. We also included the PCs of the 225 m ASTER endmember fractions and the  $9 \times 9$  SPOT texture measures. Although the previous analysis showed that models based on these variables were unlikely on their own (Appendix A), we included them in order to determine 1) whether the 0.2 and 5.06 ha scales were important when combined with other scales, and 2) if a multi-scaled RS model could outperform a single-scaled field data model. We tested 79 models representing different combinations of the four datasets and scales. Table 3 presents the information measures of the six best models, the top models

using field or RS data exclusively, and the global model, as well as descriptions of the physical meanings of the RS PCs appearing in the most likely models.

Similar to the microhabitat selection models (Table 2), the information measures of the top six models show that there is no

Table 3

Selected results of the multiple logistic regression models based on specified combinations of the field and RS data variables that provide the most likely explanation of bongo habitat selection

Rank	Model ( $R=79$ , $n=117$ )*	$K^\dagger$	Scales (ha)	$AIC_c$	$\Delta_i$	$w_i$	$R_{ss,adj}^2$
1	Shrub, Forb, GC, HH, ASTER SMA 450 PC1, PC2	7	0.04, 20.25	105.39	0.00	0.12	0.36
2	Shrub, Forb, GC, HH, ASTER SMA 450 PC2	6	0.04, 20.25	105.62	0.23	0.11	0.35
3	BA, Shrub, Forb, GC, HH, ASTER SMA 450 PC2	7	0.04, 20.25	106.85	1.46	0.06	0.35
4	Shrub, Forb, GC, HH, ASTER SMA 450 PC1-3	8	0.04, 20.25	106.96	1.57	0.05	0.36
5	Shrub, Forb, GC, HH, ASTER SMA 450 PC2, PC3	7	0.04, 20.25	107.10	1.71	0.05	0.34
6	BA, Shrub, Forb, GC, HH, ASTER SMA 450 PC1, PC2	8	0.04, 20.25	107.19	1.80	0.05	0.36
33	BA, CC, Shrub, Forb, HH	6	0.04	112.27	6.88	0.00	0.29
<b>38</b>	BA, Bamb, CC, Shrub, Forb, GC, HH, ASTER SMA 225 PC1- PC3, 450 PC1-PC3; SPOT 9×9 PC1,PC2‡	16	0.04, 0.20, 5.06, 20.25	112.32	6.93	0.00	0.45
49	ASTER SMA 450 PC1, PC2; SPOT 9×9 PC1	4	0.20, 20.25	113.70	8.31	0.00	0.27

Meaning of RS PCs:  $a$ =eigen value proportion;  $b$ =dominant eigen vectors;  $c$ =interpretation of PC gradient.

- ASTER SMA 450 PC1:  $a=0.54$ ;  $b=-0.40$  GV, 0.63 NPV, 0.67 Soil;  $c$ =Closed forest with higher stem and/or bamboo densities to shrubby, more open areas.
- ASTER SMA 450 PC2:  $a=0.30$ ;  $b=0.90$  GV, 0.41 NPV;  $c$ =Drier (conifer rich) forests to moister (often bamboo-dominated) forests.
- ASTER SMA 450 PC3:  $a=0.16$ ;  $b=-0.66$  NPV, 0.73 Soil;  $c$ =Lower elevation open or secondary forest with abundant broad-leaved shrubs and tall forbs to high altitude forest/grassland/sclerophyllous shrubland mosaic.

The results of the seven best models, the global model (denoted by the boldface, underlined model rank number) and the best RS and field data only models are presented, as well as the spatial scales they represent. Models were ranked and evaluated using the modified Akaike's Information Criterion ( $AIC_c$ ), the Akaike difference ( $\Delta_i$ ), and Akaike weights ( $w_i$ ). The adjusted sum of squares  $R^2$  ( $R_{ss,adj}^2$ ) indicates the variance in the response data explained by each model. Interpretations of the physical meanings of the principal components (PCs) of the RS variables are provided, together with their eigen values and dominant eigen vectors.

\* $R$ =number of candidate models, including the global model; BA=basal area; CC=proportion canopy cover; Shrub=shrub density; Forb=tall forb density; GC=proportion ground cover; HH=relative height of herbaceous layer. SMA 225/450=spectral mixture analysis endmember fractions aggregated to 225 or 450 m resolution; PC=principal component; 9×9=window sizes used in texture analysis.

† $K$ =number of predictors plus regression intercept.

‡Hosmer–LEMESHOW test result:  $\chi^2=3.60$   $df=8$ ,  $p<0.89$ .

clear best model, as all six have sub-two  $\Delta$  values and similar  $w$  terms. Each model also accounts for roughly the same amount of variance in the response variable ( $R_{ss,adj}^2=34$ –36%). However, another parallel between this multi-scale analysis and Section 3.2's microhabitat assessment is that the top models' common features are more telling than their variations. The six best models each consist of two fundamental elements: 1) the four micro-scale (0.04 ha) understorey structural variables; 2) at least one of the 450 m (20.25 ha) ASTER endmembers PCs, which describe gradients in patch-scale forest structure (see PC description in Table 3). The 2nd PC is the common thread in all models, and appears to contain the most essential information on patch structure because its extremes match structural types found at the upper and lower ends of the north-south precipitation gradient in the Aberdares.

In comparison, the best model comprised only of micro-habitat variables was far less likely than the hybrid RS-microhabitat models, ranked 33rd with a  $\Delta$  value of 6.88. The most likely model using RS data only was even less likely, ranked 49th with a  $\Delta$  value of 8.31. The 0.2 ha scale represented by the PCs of the SPOT 9×9 texture variables also proved to be relatively unimportant, as the top model featuring this scale was ranked 7th (SPOT PC 2, ASTER 450 PC 2, and the four understorey variables:  $\Delta_i=2.19$ ,  $w_i=0.04$ ). The same holds true of the 5.06 ha scale described by PCs of the 225 m ASTER endmember fractions, as its best model was ranked even lower at 31 (ASTER 225 PC 2, basal area, and the four understorey variables:  $\Delta_i=6.02$ ,  $w_i=0.01$ ).

These results indicate that the 0.04 ha microhabitat scales and the 20.25 ha patch scales are dominant. The former is characterized by field data variables and the latter by the 450 m resolution ASTER endmember fractions.

## 4. Discussion

### 4.1. Habitat features, scale, and RS data

The first half of our initial two-step analysis (logistic regression analysis of field-derived microhabitat variables) showed that understorey structure drives bongo habitat use at the micro-scale, as understorey variables were constant features of the most likely microhabitat selection models (Table 2). These variables are important because they directly measure browse and cover availability. This is evident in the simple univariate analysis (Table 1), which shows that bongos prefer micro-sites with abundant tall forbs (the most heavily browsed life-form) and relatively few woody shrubs (which are generally less edible). In comparison, the influential overstorey measures (basal area, bamboo density, and canopy cover) are unlikely to directly influence bongo behavior, but have importance because they best describe the canopy conditions that foster the bongo's preferred understorey environment.

The second step (the correlation analysis) showed that the RS data could not detect these important understorey features. Optical sensors are unable to penetrate forest canopies, thus understorey variables were poorly correlated with the RS data. The two significant RS-understorey relationships (Fig. 3) found

are attributable to RS correlations with canopy variables that are in turn correlated with the understorey, rather than direct RS detection. On the other hand, forest canopy features were detected by the finer-resolution RS data with reasonable success. Although the strongest RS-canopy variable correlations showed only moderate  $r$  values, the large number of modestly strong, highly significant correlations indicates that the finer-scaled RS data discern micro-scale canopy structure characteristics. This assertion is supported by the proven ability of spectral mixture and texture analysis to measure forest structural properties (Kayitakire et al., 2006; Peddle et al., 2001; Sabol et al., 2002; Wulder et al., 1998).

This initial “two-step” analysis revealed the connection between the finer-scaled RS variables and the most influential microhabitat variables. In doing so, it enabled us to understand the physical meaning of the RS measures scaled to coarser resolutions, as many of these are either aggregates of finer-scaled variables (e.g. 105–450 m ASTER endmember fractions) or show similar correlation patterns with canopy structure (e.g. SPOT 9 × 9 and 21 × 21 texture PCs compared to 3 × 3 and 5 × 5). For instance, the 30 m ASTER endmember fractions detect micro-scale canopy structure, thus it follows that their 450 m aggregates characterize patch-scale (20.25 ha) canopy conditions.

The predictor variables used in the final logistic regression analysis therefore represent vegetation structural features at multiple spatial scales. This analysis showed that micro-scale understorey and patch-scale canopy structural properties are both important in determining bongo habitat selection. Our use of AIC<sub>c</sub> makes this finding more robust, as this method selects the most informative models while penalizing over-fitting (Burnham & Anderson, 2002). The importance of the microhabitat scale can be explained as follows: since understorey characteristics determine whether a bongo can meet its most essential needs (food, water, minerals, cover), bongos continually assess and react to such features within their immediate surroundings (i.e. at the micro-scale). Patch scale canopy structure is presumably important because it determines the abundance of preferred micro-scale understorey features available to bongos within a broader area. This multi-scale habitat selection has been seen in caribou, whose primary winter habitat is stands of sub-alpine spruce *Abies lasiocarpa*, the species of tree most likely to create caribou's preferred micro-scale forage: wind-thrown trees hosting arboreal lichen (Terry et al., 2000).

Vegetation structure at intermediate scales appears to have little influence, as the 0.2–5.06 ha scale RS variables were poor predictors of bongo habitat use. This finding reflects habitat selection rather than data discrepancies, as the particular RS variables were comparable in their relationships with canopy structure; they were either aggregates of the 30 m ASTER endmember fractions, or texture variables that were more strongly correlated with canopy variables.

We could not fully assess the importance of vegetation structure at scales larger than 20.25 ha, because MODIS data were poor predictors of bongo habitat selection (Appendix A), and cloud cover in the ASTER scene precluded aggregations

coarser than 450 m. Although MODIS is comparable to ASTER in spectral depth, and showed significant correlations with several canopy structure measures, the rugged terrain presumably caused it to fail as a predictor. In the highly dissected Aberdares, the MODIS sensor captures topographical as well as vegetation features. In contrast, the 30 m resolution ASTER signal is dominated by vegetation, thus aggregated ASTER pixels provide truer estimates of patch-scale canopy structure, which influences bongos more than slope or aspect variations.

ASTER and SPOT are most suited for detecting the habitat features that are ecologically relevant to the bongo. Panchromatic SPOT data correlates most strongly with fine-scale canopy structure (except bamboo density), but ASTER is more useful because its nine bands and multiple resolutions capture information in both the spatial and spectral domains. Band 4 (1.60–1.70 μm) is presumably one of ASTER's greatest advantages, as its LANDSAT equivalent (Band 5) has been shown to be particularly important for discriminating forest structural features (Lu et al., 2004).

#### 4.2. Implications for ongoing ecological research and bongo conservation

RS data allowed us to identify important patch-scale structural features that we could not feasibly record in the field. We derived these patch-scale RS variables using spectral mixture analysis, which is a more transportable technique because it is directly related to forest structural properties (Sabol et al., 2002), and should thus be less sensitive to area-specific variations that can cause other techniques (e.g. NDVI) to produce widely differing values for similar features. This bodes well for mapping patch-scale canopy structure in other bongo habitats (e.g. Mount Kenya) where field calibration data are unavailable.

It will be harder to use RS data to map predictors at the important microhabitat scale. The correlation analysis suggests it is possible to develop reasonably accurate quantitative relationships between RS data and canopy structure, provided that multiple RS measures are used to minimize error. However, the crucial understorey features cannot be mapped using optical RS data. More sophisticated active or hyperspectral sensors could perhaps overcome this problem. LIDAR and synthetic aperture radar can measure three-dimensional structure (Hyde et al., 2006), and may thus correlate more strongly with understorey features. Hyperspectral RS has been used to detect an invasive understorey herb by measuring its impact on the foliar chemistry and water content of canopy trees (Asner & Vitousek, 2005). However, such tools tend to be costly and are relatively unavailable in East Africa.

We must therefore rely on the existing RS data to derive reasonable approximations of understorey structure. It may be possible to model overstorey–understorey associations, and use these relationships with RS-derived canopy structure measures to map understorey features. Another approach is to compress canopy and understorey structural variables into indices and use RS to map index values. Structural indices are widely used in forest ecology (e.g. McElhinny et al., 2006; Neumann &

Starlinger, 2001; Pommerening 2002), and have been successfully employed to relate RS data to forest structure (Cohen & Spies, 1992; Hansen et al., 2001) and to characterize mammalian and avian habitats (Coops & Catling, 2002; Gibson et al., 2004).

#### 4.3. Potential shortcomings

The relatively small sample size and the distribution of the collected bongo plots raise the possibility of bias, and that our models present a flawed picture of bongo habitat use. Conservation surveys of rare species are notoriously biased, as they are often improperly randomized and/or stratified (Guisan et al., 2006). We concede that RS data limitations prevented us from evaluating scales coarser than 20.25 ha, but contend that the spatio-temporal distribution of our samples adequately captures bongo distribution and the range of forest structural types in the study area. We sampled widely throughout the Aberdares, using a design that 1) was effectively random in relation to the landscape (the grid point system), and 2) accounted for altitudinal and precipitation gradients. Our surveys covered most of the areas occupied by the main surviving bongo herds, as well as many areas where bongos were not found. Although our bongo samples were often closely-spaced (see Fig. 1 and Section 2.2.2), these plots were collected over three seasons within apparent home ranges, the continued use of which has been confirmed during subsequent surveys by our colleagues. These data were thus collected within preferred bongo habitat, which is supported by the fact that these areas are largely comprised of the sort of herb-rich open and secondary forests that bongos are believed to favor (Kingdon, 1982; Klaus-Hugi et al., 2000).

Historically, bongos were more widely distributed throughout the Aberdares (Kingdon, 1982; Prettejohn, 2004), which suggests that the few remaining bongos do not utilize all suitable habitat areas. Our “non-bongo” grid samples therefore do not necessarily represent true bongo absence. This possibility suggests that our models were more likely to be conservative in discriminating influential habitat features, rather than erroneous.

This study focused on the relationship between bongo and vegetation structure, and therefore did not include other factors that are likely to affect bongo habitat selection. The level of human presence is an example of a factor that appears to particularly influence bongos. The role of such factors should be investigated and incorporated in subsequent distribution models.

#### 4.4. Implications for the study of other rare animals

This study should interest ecologists and conservation biologists studying other mobile, forest-dwelling species, particularly where rarity and environment combine to make field surveys difficult. Remote sensing is an important tool to aid species distribution modeling in such circumstances (Rushton et al., 2004), but the more promising remote sensing techniques are usually not employed by ecologists (Turner et al., 2003). There appears to be two broad classes of RS-based ecological studies, divided into those undertaken by remote sensing experts and those undertaken by applied ecologists. In

the former case, an advanced RS technique is used to identify habitat features of potential importance for certain organisms, but the authors typically do not use the method to identify the organism's habitat requirements or distributions (e.g. Hyde et al., 2006, Theau et al., 2005). In the second category, ecologists use RS to provide more basic (and fairly limited) input for distribution models, usually in the form of categorical predictors (e.g. Schadt et al., 2002) or simple indices such as NDVI (e.g. Osborne et al., 2001). Several recent studies have generated continuous predictors for distribution models by regressing RS data against field-collected habitat variables (e.g. Gibson et al., 2004; Jeganathan et al., 2004). However, such studies are still relatively rare, and the underlying regression techniques are fairly simple and depend on substantial field calibration data to be transported to other habitats.

Our study helps to address the gap between applied ecology and remote sensing, as it shows how more advanced RS analysis techniques can be used in habitat modeling. It also contributes by providing further insight into 1) the ability of RS data to quantify habitat structure, and 2) the performance of several optical RS datasets in an environment that promotes detection errors. Our use of the information theoretic approach makes this study more relevant to ecologists, who increasingly prefer this methodology for habitat modeling studies (Burnham & Anderson, 2002; Rushton et al., 2004).

## 5. Conclusions

This analysis confirmed our hypothesis that bongo habitat is defined at multiple spatial scales. We found that forest understorey characteristics at the micro-scale and canopy structural conditions at a patch-scale of ~20 ha are important in determining bongo habitat, but further work is needed to assess the importance of coarser scales. Future distribution models must incorporate multi-scaled predictors if suitable bongo habitat is to be accurately identified, as models representing different, single scales can generate different distribution patterns (Wiens, 1989).

The validation of our hypothesis is an important first step in understanding bongo ecology, given the near-absence of existing information and the difficulty of studying this animal. Our methodology improves our confidence in the legitimacy of our central finding: we allied field and RS data analyzed with techniques more advanced than those typically used in ecological modeling studies with the information theoretic approach to model selection, which provides more ecologically sound models than those based on conventional null-hypothesis testing (Burnham & Anderson, 2002). These procedures also provide valuable insight into how RS benefits ecological studies of rare species.

Our “two-step” approach (Jeganathan et al., 2004) related multi-scaled RS variables to important microhabitat variables, which allowed us to distinguish larger-scaled forest structural properties that we could not detect from the ground. This approach is an alternative to the well-stratified, multi-scaled field surveys recommended for distribution modeling studies (Vaughan & Ormerod, 2003). Such surveys are typically beyond the means of most ecologists, and are unlikely to yield sufficient data on rare species (Guisan et al., 2006). These

limitations and our findings lead us to conclude that RS is indispensable for habitat modeling studies of the bongo and similar rare, mobile species, given the multi-scaled nature of habitat use and the superior scalability of RS data compared to field data. ASTER is particularly well-suited for this task, as its spectral range and multiple resolutions permit the derivation of scalable, sub-pixel estimates of vegetation, as well as information on the spatial configuration of habitats.

Our study also shows that optical RS cannot replace field data in characterizing micro-scale habitat structure, particularly the understorey features important to a rare, mobile forest herbivore. RS data can measure the micro-scale canopy features responsible for shaping understorey conditions, which suggests it is possible to approximate the understorey environment using forest structural indices or other modeling approaches. However, our results emphasize the importance of using field and RS data together when modeling rare species' habitat use (Jeganathan et al., 2004; Rushton et al., 2004). Field data are needed to identify important habitat features and to ascribe physical meaning to RS data, which enable habitat variables to be extensively mapped at a variety of spatial scales. Spectral mixture analysis is a more profitable technique to use when field data are limited, as its direct connection to forest properties permits RS-based habitat models that need less calibration than more direct habitat-reflectance models.

### Acknowledgements

We thank the former and current Senior Wardens of Aberdare National Park, Anne Kahihia and Catherine Wambani, and the Assistant Director Joseph Warutere for their support for this research. Assistant Warden Gichohi is thanked for his assistance in organizing permits and personnel. The Ranger staff of the Aberdare National Park provided protection for the field team. The former Director of Biodiversity, Ecosystems and Research for the Kenya Wildlife Service, Dr. Richard Bagine, provided the necessary approval for this research project. The Bongo Surveillance Team (Michael Prettejohn, Joseph Kariuki, Matthew Gichuri, Kiragu Gichuri, Boniface Nderitu, Peter Mwangi, Stanley Gichure, Laban Kariuki, and Josphat Korage) provided tracking expertise and crucial field support. Jessica and Henry Henley and Francis Maina provided accommodation and expedition assistance. Mitochondrial DNA analysis was undertaken by Jacquelyn Bishop of the University of Cape Town, Dorcas Kavembe, Joseph Jung'a, and Charles Kimwele of the University of Nairobi, and Katherine Dunbar, Patricia Faria, and Michael Bruford of Cardiff University. Additional assistance was provided by Colin Church of the Rhino Ark Foundation, Olivier Hanotte and Dorine Adhoch of the International Livestock Research Institute, and Christian Lambrechts of the United Nations Environmental Programme. Paul Reillo of the Rare Species Conservatory Foundation conceived and implemented the Bongo Repatriation and Reintroduction Programme, and made this research program possible. This work was supported by NASA Headquarters under the Earth System Science Fellowship Grant NNG05GR43H. Additional

funding was provided by the Wildlife Conservation Society (Conservation Research Fellowship), the Explorers Club Washington Group (Exploration and Field Research Grant), and the University of Virginia's Department of Environmental Science. John Porter, David Richardson, Robert Washington-Allen, David Carr, Henry Wilbur, Richard Estes, and Anna Estes provided valuable input into the methodology and presentation of this research.

### Appendix A

Selected results of the multiple logistic regression models employing RS-derived predictor variables segregated by sensor type and scale. The results of the five best models, the highest ranked models from each individual dataset, and the global model (denoted by the boldface, underlined model rank) are presented, as well as the spatial scales they represent. Models were ranked and evaluated using the modified Akaike's Information Criterion (AIC<sub>c</sub>), the Akaike difference (Δ<sub>i</sub>), and Akaike weights (w<sub>i</sub>). The adjusted sum of squares R<sup>2</sup> (R<sup>2</sup><sub>ss,adj</sub>) indicates the proportion of variance explained in the response

Rank	Model (R=50, n=117)*	K <sup>†</sup>	Scale (ha)	AIC <sub>c</sub>	Δ <sub>i</sub>	w <sub>i</sub>	R <sup>2</sup> <sub>ss,adj</sub>
1	ASTER SMA 450 PC1, PC2	3	20.25	113.32	0.00	0.72	0.26
2	ASTER SMA 450 PC1, PC2, PC3	4	20.25	115.27	1.94	0.27	0.25
3	ASTER SMA 450 PC2, PC3	3	20.25	125.64	12.32	0.00	0.16
4	ASTER SMA 225 PC1, PC2	3	5.06	127.72	14.39	0.00	0.16
5	ASTER SMA 225 PC1, PC2, PC3	4	5.06	128.88	15.55	0.00	0.15
6	SPOT 9×9 Texture PC1, PC2	3	0.20	129.64	16.31	0.00	0.15
8	SPOT 21×21 PC1, PC2	3	1.10	133.16	19.83	0.00	0.13
9	SPOT 5×5 PC1, PC2	3	0.06	134.09	20.76	0.00	0.10
10	ASTER SMA 105 PC1, PC2	3	1.10	134.24	20.91	0.00	0.11
12	ASTER SMA 30 PC2, PC3	3	0.09	134.36	21.04	0.00	0.11
14	SPOT 3×3 PC1, PC2	3	0.02	135.16	21.84	0.00	0.09
17	ASTER VNIR 3×3 PC1, PC2, PC3	4	0.20	135.61	22.29	0.00	0.09
18	MODIS 927 PC2, PC3	3	85.93	135.88	22.56	0.00	0.07
19	ASTER VNIR 7×7 PC1, PC2, PC3	4	1.10	136.52	23.19	0.00	0.08
22	MODIS 463 PC1, PC3	3	21.44	136.93	23.61	0.00	0.06
<b>50</b>	ASTER: 1) SMA: 30 m (PC1-3), 105 m (PC1-3), 225 m (PC1-3), 450 m (PC1-3); 2) VNIR Texture: 3×3 (PC1-5), 7×7 (PC1-5). MODIS SMA: 463 m (PC1-3); 927 m (PC1-3). SPOT Texture: 3×3 (PC1-3); 5×5 (PC1-2); 9×9 (PC1-2); 21×21 (PC1-2) ‡	38	0.02–85.93	166.36	53.03	0.00	0.47

\*R=number of candidate models, including the global model; SMA=spectral mixture analysis; PC=principal component; 3×3, 5×5, 7×7, 9×9, 21×21=window sizes used in texture analyses.

†K=number of predictors plus regression intercept.

‡Hosmer–Lemeshow test result: (χ<sup>2</sup>=7.16, df=7, p<0.41).

### References

Adams, J. B., Smith, M. O., & Gillespie, A. R. (1989). Simple models for complex natural surfaces: a strategy for the hyperspectral era of remote sensing. *Proceedings of the International Geoscience and Remote Sensing Symposium (IGARSS'89) 12th Canadian Symposium on Remote Sensing* (pp. 16–21).

- Asner, G. P., & Vitousek, P. M. (2005). Remote analysis of biological invasion and biogeochemical change. *Proceedings of the National Academy of Sciences of the United States of America*, 102(12), 4383–4386.
- Baraldi, A., & Parmiggiani, F. (1995). An investigation of the textural characteristics associated with gray level co-occurrence matrix statistical parameters. *IEEE Transactions on Geoscience and Remote Sensing*, 33(2), 293–304.
- Brown, J. H. (1995). *Macroecology*. Chicago: The University of Chicago Press.
- Burnham, K. P., & Anderson, D. R. (2002). *Model selection and multimodel inference*, (2nd ed.). New York: Springer-Verlag.
- Bussmann, R. W. (1994). *The forests of Mount Kenya: vegetation, ecology, destruction and management of a tropical mountain forest ecosystem*. Bayreuth: Universität Bayreuth Doctorate Edition.
- Cassing, G., Greenberg, L. A., & Mikusinski, G. (2006). Moose (*Alces alces*) browsing in young forest stands in Central Sweden: a multiscale perspective. *Scandinavian Journal of Forest Research*, 21(3), 221–230.
- Coburn, C.A. 2006. Off-nadir adjustment to SCS+C correction. Personal communication.
- Cohen, W. B., & Spies, T. A. (1992). Estimating structural attributes of douglas-fir/western hemlock forest stands from Landsat and SPOT imagery. *Remote Sensing of Environment*, 41(1), 1–17.
- Coops, N. C., & Catling, P. C. (2002). Prediction of the spatial distribution and relative abundance of ground-dwelling mammals using remote sensing imagery and simulation models. *Landscape Ecology*, 17(2), 173–188.
- Debinski, D. M., Kindscher, K., & Jakubauskas, M. E. (1999). A remote sensing and GIS-based model of habitats and biodiversity in the Greater Yellowstone ecosystem. *International Journal of Remote Sensing*, 20(17), 3281–3291.
- Dunn, J. E. (1978). Optimal sampling in radio telemetry studies of home range. In H. H. Shugart (Ed.), *Time series and ecological processes: Proceedings of a SIMS conference*.
- Elkan, P. W. (2003). Ecology and conservation of bongo antelope (*Tragelaphus eurycerus*) in Lowland Forest, Northern Republic of Congo. St. Paul: University of Minnesota PhD Edition.
- ENVI. (2006). *Environment for visualizing images*. Boulder, CO, USA: ITT Visual Information Solutions.
- Estes, R. D. (1974). Social organization of the African Bovidae. *Proceedings of an international symposium on the behavior of ungulates and its relation to management* (pp. 166–205). Morges, Switzerland: IUCN Special Publication (New Series) No. 24.
- Estes, R. D. (1991). *The behavior guide to african mammals*. Berkeley: University of California Press.
- Fisher, J. T., Boutin, S., & Hannon, a. S. J. (2005). The protean relationship between boreal forest landscape structure and red squirrel distribution at multiple spatial scales. *Landscape Ecology*, 20(1), 73–82.
- Gathaara, G. N. (1999). Aerial survey of the destruction of Mount Kenya, Imenti, and Ngare Ndare Forest Reserves. Nairobi, Kenya: Kenya Wildlife Service.
- Gibson, L. A., Wilson, B. A., Cahill, D. M., & Hill, J. (2004). Spatial prediction of rufous bristlebird habitat in a coastal heathland: a GIS-based approach. *Journal of Applied Ecology*, 41(2), 213–223.
- Graf, R. F., Bollmann, K., Suter, W., & Bugmann, H. (2005). The importance of spatial scale in habitat models: Capercaillie in the Swiss Alps. *Landscape Ecology*, 20(6), 703–717.
- Gu, D., & Gillespie, A. (1998). Topographic normalization of landsat TM images of forest based on subpixel sun-canopy-sensor geometry. *Remote Sensing of Environment*, 64(2), 166–175.
- Guisan, A., Broennimann, O., Engler, R., Vust, M., Yoccoz, N. G., Lehmann, A., et al. (2006). Using niche-based models to improve the sampling of rare species. *Conservation Biology*, 20(2), 501–511.
- Guisan, A., & Zimmermann, N. E. (2000). Predictive habitat distribution models in ecology. *Ecological Modelling*, 135(2–3), 147–186.
- Hansen, M. J., Franklin, S. E., Woudsma, C., & Peterson, M. (2001). Forest structure classification in the North Columbia mountains using the Landsat TM tasseled cap wetness component. *Canadian Journal of Remote Sensing*, 27(1), 20–32.
- Hillman, J. C. (1986). Aspects of the biology of the bongo antelope, *Tragelaphus eurycerus* (Ogilby 1837) in Southwest Sudan. *Biological Conservation*, 38(3), 255–272.
- Hillman, J. C., & Gwynne, M. D. (1987). Feeding of the bongo antelope, *Tragelaphus eurycerus* (Ogilby, 1837), in Southwest Sudan. *Mammalia*, 51(1), 53–63.
- Holm, S. (1979). A simple sequentially rejective multiple test procedure. *Scandinavian Journal of Statistics*, 6, 65–70.
- Hosmer, D. W., & Lemeshow, S. (1989). *Applied logistic regression*. New York: Wiley.
- Hudak, A. T., Lefsky, M. A., Cohen, W. B., & Berterretche, M. (2002). Integration of LiDAR and Landsat ETM plus data for estimating and mapping forest canopy height. *Remote Sensing of Environment*, 82(2–3), 397–416.
- Hyde, P., Dubayah, R., Walker, W., Blair, J. B., Hofton, M., & Hunsaker, C. (2006). Mapping forest structure for wildlife habitat analysis using multi-sensor (LiDAR, SAR/InSAR, ETM+, quickbird) synergy. *Remote Sensing of Environment*, 102(1–2), 63–73.
- Imbernon, J. (1999). Pattern and development of land-use changes in the Kenyan Highlands since the 1950s. *Agriculture Ecosystems & Environment*, 76(1), 67–73.
- James, F. C., & Shugart, H. H. (1970). A quantitative method of habitat description. *Audubon Field Notes*, 24(6), 727–736.
- Jeganathan, P., Green, R. E., Norris, K., Vogiatzakis, I. N., Bartsch, A., Wotton, S. R., et al. (2004). Modelling habitat selection and distribution of the critically endangered Jerdon's courser *Rhinoptilus bitorquatus* in scrub jungle: an application of a new tracking method. *Journal of Applied Ecology*, 41(2), 224–237.
- Jensen, J. R. (1996). *Introductory digital image processing*, (2nd ed.). Upper Saddle River, NJ, USA: Prentice-Hall Inc.
- Johnson, C. J., Seip, D. R., & Boyce, M. S. (2004). A quantitative approach to conservation planning: using resource selection functions to map the distribution of mountain caribou at multiple spatial scales. *Journal of Applied Ecology*, 41(2), 238–251.
- Kayitakire, F., Hamel, C., & Defourny, P. (2006). Retrieving forest structure variables based on image texture analysis and IKONOS-2 imagery. *Remote Sensing of Environment*, 102(3–4), 390–401.
- Kerr, J. T., & Ostrovsky, M. (2003). From space to species: ecological applications for remote sensing. *Trends in Ecology & Evolution*, 18(6), 299–305.
- Kingdon, J. (1982). *East African mammals: An atlas of evolution in Africa*. New York: Academic Press.
- Klaus, G., Klaus-Hugi, C., & Schmid, B. (1998). Geophagy by large mammals at natural licks in the rain forest of the Dzanga National Park, Central African Republic. *Journal of Tropical Ecology*, 14, 829–839.
- Klaus-Hugi, C., Klaus, G., & Schmid, B. (2000). Movement patterns and home range of the bongo (*Tragelaphus eurycerus*) in the rain forest of the Dzanga National Park, Central African Republic. *African Journal of Ecology*, 38(1), 53–61.
- Klaus-Hugi, C., Klaus, G., Schmid, B., & Konig, B. (1999). Feeding ecology of a large social antelope in the rainforest. *Oecologia*, 119(1), 81–90.
- Kock, R. A., Wambua, J. M., Mwanja, J., Wamwayi, H., Ndungu, E. K., Barrett, T., et al. (1999). Rinderpest epidemic in wild ruminants in Kenya 1993–97. *Veterinary Record*, 145(10), 275–283.
- KWS (2006). Kenya wildlife service national parks and reserves. [www.kws.org/parks.html](http://www.kws.org/parks.html)
- Lambrechts, C., Woodley, B., Church, C., & Gachanja, M. (2003). Aerial survey of the destruction of the Aberdare Range forests. Nairobi, Kenya: UNEP, KWS, Rhino Ark, KFWG.
- Lu, D. S., Mausel, P., Brondizio, E., & Moran, E. (2004). Relationships between forest stand parameters and Landsat TM spectral responses in the Brazilian Amazon basin. *Forest Ecology and Management*, 198(1–3), 149–167.
- Lu, D. S., Moran, E., & Batistella, M. (2003). Linear mixture model applied to Amazonian vegetation classification. *Remote Sensing of Environment*, 87(4), 456–469.
- Maier, J. A. K., Hoef, J. M. V., McGuire, A. D., Bowyer, R. T., Saperstein, L., & Maier, H. A. (2005). Distribution and density of moose in relation to landscape characteristics: effects of scale. *Canadian Journal of Forest Research-Revue Canadienne De Recherche Forestiere*, 35(9), 2233–2243.
- McElhinny, C., Gibbons, P., & Brack, C. (2006). An objective and quantitative methodology for constructing an index of stand structural complexity. *Forest Ecology and Management*, 235(1–3), 54–71.

- Mittlbock, M., & Schemper, M. (1999). Computing measures of explained variation for logistic regression models. *Computer Methods and Programs in Biomedicine*, 58(1), 17–24.
- Morin, P., Berteaux, D., & Klvana, I. (2005). Hierarchical habitat selection by North American porcupines in southern boreal forest. *Canadian Journal of Zoology-Revue Canadienne De Zoologie*, 83(10), 1333–1342.
- Neumann, M., & Starlinger, F. (2001). The significance of different indices for stand structure and diversity in forests. *Forest Ecology and Management*, 145(1–2), 91–106.
- Osborne, P. E., Alonso, J. C., & Bryant, R. G. (2001). Modelling landscape-scale habitat use using GIS and remote sensing: a case study with great bustards. *Journal of Applied Ecology*, 38(2), 458–471.
- Peddle, D. R., Brunke, S. P., & Hall, F. G. (2001). A comparison of spectral mixture analysis and ten vegetation indices for estimating boreal forest biophysical information from airborne data. *Canadian Journal of Remote Sensing*, 27(6), 627–635.
- Peddle, D. R., Johnson, R. L., Cihlar, J., & Latifovic, R. (2004). Large area forest classification and biophysical parameter estimation using the 5-scale canopy reflectance model in multiple-forward-mode. *Remote Sensing of Environment*, 89(2), 252–263.
- Pommerening, A. (2002). Approaches to quantifying forest structures. *Forestry*, 75(3), 305–324.
- Prettejohn, M. (2004). Encounters with the bongo. *Swara*, 27(1), 28–30.
- Reillo, P. (2002). Repatriation of mountain bongo to Kenya. *Antelope Specialist Group Gnuletter*, 21(2), 11–15.
- Rhino-Ark (2006). Arkive: newsletter of the Rhino Ark charitable trust. 28. [www.rhinoark.org/downloads/arkive-april2006.pdf](http://www.rhinoark.org/downloads/arkive-april2006.pdf)
- Roberts, D. A., Gardner, M., Church, R., Ustin, S., Scheer, G., & Green, R. O. (1998). Mapping chaparral in the Santa Monica mountains using multiple endmember spectral mixture models. *Remote Sensing of Environment*, 65(3), 267–279.
- Rushton, S. P., Ormerod, S. J., & Kerby, G. (2004). New paradigms for modelling species distributions? *Journal of Applied Ecology*, 41(2), 193–200.
- Sabol, D. E., Gillespie, A. R., Adams, J. B., Smith, M. O., & Tucker, C. J. (2002). Structural stage in Pacific Northwest forests estimated using simple mixing models of multispectral images. *Remote Sensing of Environment*, 80(1), 1–16.
- Saveraid, E. H., Debinski, D. M., Kindscher, K., & Jakubauskas, M. E. (2001). A comparison of satellite data and landscape variables in predicting bird species occurrences in the Greater Yellowstone ecosystem, USA. *Landscape Ecology*, 16(1), 71–83.
- Scarth, P., Phinn, S. R., & McAlpine, C. (2001). Integrating high and moderate spatial resolution image data to estimate forest age structure. *Canadian Journal of Remote Sensing*, 27(2), 129–142.
- Schadt, S., Revilla, E., Wiegand, T., Knauer, F., Kaczensky, P., Breitenmoser, U., et al. (2002). Assessing the suitability of Central European landscapes for the reintroduction of Eurasian lynx. *Journal of Applied Ecology*, 39(2), 189–203.
- Schmitt, K. (1991). The vegetation of the Aberdare National Park, Kenya. Innsbruck: Universitätsverlag Wagner.
- Smith, A. M. S. (2006). How to convert ASTER radiance values to reflectance: an online guide. University of Idaho. [www.cnrhome.uidaho.edu/default.aspx?pid=85984](http://www.cnrhome.uidaho.edu/default.aspx?pid=85984)
- Soenen, S. A., Peddle, D. R., & Coburn, C. A. (2005). SCS+C: a modified sun-canopy-sensor topographic correction in forested terrain. *IEEE Transactions on Geoscience and Remote Sensing*, 43(9), 2148–2159.
- Soule, M. E. (1986). Conservation biology and the real world. In M. E. Soule (Ed.), *Conservation biology: The science of scarcity and diversity* (pp. 1–12). Sunderland, Massachusetts: Sinauer Associates, Inc.
- St-Louis, V., Pidgeon, A. M., Radeloff, V. C., Hawbaker, T. J., & Clayton, M. K. (2006). High-resolution image texture as a predictor of bird species richness. *Remote Sensing of Environment*, 105, 299–312.
- Terry, E. L., Mclellan, B. N., & Watts, G. S. (2000). Winter habitat ecology of mountain caribou in relation to forest management. *Journal of Applied Ecology*, 37(4), 589–602.
- Theau, J., Peddle, D. R., & Duguay, C. R. (2005). Mapping lichen in a caribou habitat of Northern Quebec, Canada, using an enhancement-classification method and spectral mixture analysis. *Remote Sensing of Environment*, 94(2), 232–243.
- Trexler, J. C., & Travis, J. (1993). Nontraditional regression analyses. *Ecology*, 74(6), 1629–1637.
- Tucker, C. J., Grant, D. M., & Dykstra, J. D. (2004). NASA's global orthorectified Landsat data set. *Photogrammetric Engineering and Remote Sensing*, 70(3), 313–322.
- Turkalo, A., & Klaus-Hugi, C. (1999). Group size and group composition of the bongo (*Tragelaphus eurycerus*) at a natural lick in the Dzanga National Park, Central African Republic. *Mammalia*, 63(4), 437–447.
- Turner, W., Spector, S., Gardiner, N., Fladeland, M., Sterling, E., & Steininger, M. (2003). Remote sensing for biodiversity science and conservation. *Trends in Ecology & Evolution*, 18(6), 306–314.
- Vaughan, I. P., & Ormerod, S. J. (2003). Improving the quality of distribution models for conservation by addressing shortcomings in the field collection of training data. *Conservation Biology*, 17(6), 1601–1611.
- Walsh, P. D., & White, L. J. T. (1999). What it will take to monitor forest elephant populations. *Conservation Biology*, 13(5), 1194–1202.
- Wiens, J. A. (1989). Spatial scaling in ecology. *Functional Ecology*, 3(4), 385–397.
- Wulder, M. A., Hall, R. J., Coops, N. C., & Franklin, S. E. (2004). High spatial resolution remotely sensed data for ecosystem characterization. *Bioscience*, 54(6), 511–521.
- Wulder, M. A., LeDrew, E. F., Franklin, S. E., & Lavigne, M. B. (1998). Aerial image texture information in the estimation of northern deciduous and mixed wood forest leaf area index (LAI). *Remote Sensing of Environment*, 64(1), 64–76.